

7207010148 920626
PDR ADDCK 05000339
P PDR

TECHNICAL REPORT NE-876 - Rev. 0

NORTH ANNA UNIT 2, CYCLE 8
CORE PERFORMANCE REPORT

NUCLEAR ANALYSIS AND FUEL
POWER ENGINEERING SERVICES
VIRGINIA POWER
MAY, 1992

PREPARED BY: T. T. Nguyen
T. T. Nguyen

5/20/92
Date

REVIEWED BY: T. S. Psuik
T. S. Psuik

5/20/92
Date

REVIEWED BY: T. A. Brookmire
T. A. Brookmire

5-28-92
Date

REVIEWED BY: A. P. Main
A. P. Main

5-27-92
Date

APPROVED BY: D. Dziedzisz
D. Dziedzisz

5-29-92
Date

QA Category: Nuclear Safety Related

Keywords: N2C8, Core Performance

TABLE OF CONTENTS

	PAGE
Table of Contents	1
List of Tables	2
List of Figures.	3
Section 1 Introduction and Summary.	5
Section 2 Burnup.	12
Section 3 Reactivity Depletion.	23
Section 4 Power Distribution.	25
Section 5 Primary Coolant Activity.	45
Section 6 Conclusions	50
Section 7 References.	51

LIST OF TABLES

TABLE	TITLE	PAGE
4.1	Summary of Flux Maps for Routine Operation	29

LIST OF FIGURES

FIGURE	TITLE	PAGE
1.1	Core Loading Map	8
1.2	Burnable Poison and Source Assembly Locations.	9
1.3	Movable Detector Locations	10
1.4	Control Rod Locations.	11
2.1	Core Burnup History	14
2.2	Monthly Average Load Factors	15
2.3	Assemblywise Accumulated Burnup: Measured and Predicted . . .	16
2.4	Assemblywise Accumulated Burnup: Comparison of Measured and Predicted	17
2.5A	Sub-Batch Burnup Sharing	18
2.5B	Sub-Batch Burnup Sharing	19
2.5C	Sub-Batch Burnup Sharing	20
2.5D	Sub-Batch Burnup Sharing	21
2.5E	Sub-Batch Burnup Sharing	22
3.1	Critical Boron Concentration versus Burnup - HFP-ARO	24
4.1	Assemblywise Power Distribution - N2-8-07	30
4.2	Assemblywise Power Distribution - N2-8-14	31
4.3	Assemblywise Power Distribution - N2-8-25	32
4.4	Hot Channel Factor Normalized Operating Envelope	33
4.5	Heat Flux Hot Channel Factor, $F_Q(Z)$ - N2-8-07	34
4.6	Heat Flux Hot Channel Factor, $F_Q(Z)$ - N2-8-14	35
4.7	Heat Flux Hot Channel Factor, $F_Q(Z)$ - N2-8-25	36
4.8	Maximum Heat Flux Hot Channel Factor, $F_Q(Z)*P$, vs. Axial Position	37

LIST OF FIGURES CONT'D

FIGURE	TITLE	PAGE
4.9	Maximum Heat Flux Hot Channel Factor, $F_Q(Z)$, vs. Burnup . . .	38
4.10	Maximum Enthalpy Rise Hot Channel Factor, $F\text{-delta-H}$ vs. Burnup	39
4.11	Target Delta Flux versus Burnup	40
4.12	Core Average Axial Power Distribution - N2-8-07	41
4.13	Core Average Axial Power Distribution - N2-8-14	42
4.14	Core Average Axial Power Distribution - N2-8-25	43
4.15	Core Average Axial Peaking Factor vs. Burnup	44
5.1	Dose Equivalent I-131 vs. Time	48
5.2	I-131/I-133 Activity Ratio vs. Time	49

Section 1

INTRODUCTION AND SUMMARY

On February 26, 1992, North Anna Unit 2 completed Cycle 8. Since the initial criticality of Cycle 8 on November 1, 1990, the reactor core produced approximately 1.0862×10^8 MBTU (18,239 Megawatt days per metric ton of contained uranium). The purpose of this report is to present an analysis of the core performance for routine operation during Cycle 8. The physics tests that were performed during the startup of this cycle were covered in the North Anna Unit 2, Cycle 8 Startup Physics Test Report¹ and, therefore, will not be included here.

North Anna Unit 2 was in coastdown from January 14, 1992, at which time the burnup was approximately 16,829 MWD/MTU. The coastdown accounted for an additional core burnup of roughly 1,410 MWD/MTU from the end of full power reactivity.

The Cycle 8 core consisted of 14 sub-batches of fuel: four once-burned batches from Cycle 7 (batches 9A, 9B, N1/10A, and N1/10B); seven twice-burned batches, one from North Anna 1 Cycles 3 and 4 (batch N1/5), one from North Anna 2 Cycle 5 and North Anna 1 Cycle 4 (batch N1/6), one from North Anna 1 Cycles 5 and 6 (batch N1/7), one from North Anna 2 Cycles 2 and 3 (batch 4), one from North Anna 2 Cycles 3 and 4 (batch 5A), and two from North Anna 2 Cycles 6 and 7 (batches 8A and 8B); one

thrice-burned batch from North Anna 2 Cycles 5,6, and 7 (batch 7A); and two fresh batches (batches 10A and 10B). The North Anna 2 Cycle 8 core loading map specifying the fuel batch identification, and fuel assembly locations is shown in Figure 1.1. The burnable poison locations and source assembly locations is shown in Figure 1.2. Movable detector locations are shown in Figure 1.3. Control rod locations are shown in Figure 1.4.

Routine core follow involves the analysis of four principal performance indicators. These are burnup distribution, reactivity depletion, power distribution, and primary coolant activity. The core burnup distribution is followed to verify both burnup symmetry and proper batch burnup sharing, thereby ensuring that the fuel held over for the next cycle will be compatible with the new fuel that is inserted. Reactivity depletion is monitored to detect the existence of any abnormal reactivity behavior, to determine if the core is depleting as designed, and to indicate at what burnup level refueling will be required. Core power distribution follow includes the monitoring of nuclear hot channel factors to verify that they are within the Technical Specifications² limits, thereby ensuring that adequate margins for linear power density and critical heat flux thermal limits are maintained. Lastly, as part of normal core follow, the primary coolant activity is monitored to verify that the dose equivalent iodine-131 concentration is within the limits specified by the North Anna Unit 2 Technical Specifications². A radioiodine analysis based on the iodine-131 concentration in the coolant is performed to assess the integrity of the fuel.

Each of the four performance indicators is discussed in detail for the North Anna Unit 2, Cycle 8 core in the body of this report. The results are summarized below:

1. Burnup - The burnup tilt (deviation from quadrant symmetry) on the core was no greater than $\pm 0.30\%$ with the burnup accumulation in each batch deviating from design prediction by no more than 1.69% .

2. Reactivity Depletion - The critical boron concentration, used to monitor reactivity depletion, was consistently within $\pm 0.39\% \Delta K/K$ of the design prediction which is within the $\pm 1\% \Delta K/K$ margin allowed by Section 4.1.1.1.2 of the Technical Specifications.

3. Power Distribution - Incore flux maps taken each month indicated that the assemblywise radial power distributions deviated from the design predictions by a maximum average difference of 2.5% . All hot channel factors met their respective Technical Specifications limits.

4. Primary Coolant Activity - The average dose equivalent iodine-131 activity level in the primary coolant during Cycle 8 was approximately $0.0242 \mu\text{Ci/gm}$. This corresponds to less than 3% of the operating limit for the concentration of radioiodine in the primary coolant. Radioiodine analysis indicated several fuel rod defects, which prompted ultrasonic testing (UT) during the Cycle 8 to Cycle 9 refueling outage. During UT testing, it was confirmed that eight fuel rods in five fuel assemblies were defective.

Figure 1.1
NORTH ANNA UNIT 2 - CYCLE 8
CORE LOADING MAP

FUEL ASSEMBLY DESIGN PARAMETERS

	SUB-BATCH													
	N1/5	N1/6	N1/7	N1/10A	N1/103	4	5A	7A	8A	8B	9A	9B	10A	10B
INITIAL ENRICHMENT (W/U U-235)	3.40	3.59	3.60	3.80	4.00	3.41	3.59	3.60	3.79	4.00	3.80	4.01	3.99	4.00
ASSEMBLY TYPE	17x17	17x17	17x17	17x17	17x17	17x17	17x17	17x17	17x17	17x17	17x17	17x17	17x17	17x17
NUMBER OF ASSEMBLIES	2	1	1	12	3	2	6	7	8	8	16	31	28	16
FUEL RODS PER ASSEMBLY	264	264	264	264	264	264	264	256	264	264	264	264	264	264

Figure 1.2
NORTH ANNA UNIT 2 - CYCLE 8
BURNABLE POISON AND SOURCE
ASSEMBLY LOCATIONS

D	P	H	S	L	K	J	H	G	F	E	B	C	B	A
														1
							4P	4P						2
							BP008	BP067						3
							7P	12P	20P	12P	7P			4
							BP014	BP024	BP066	BP023	BP016			5
							16P	20P	20P	16P				6
							BP044	BP060	BP059	BP045				7
							2P	16P	20P	16P	7P			8
							BP013	BP042	BP058	BP057	BP041	BP015		9
							12P	20P	16P	20P	12P			10
							BP022	BP056	BP032	BP031	BP055	BP021		11
							4P	20P	16P	16P	20P	4P		12
							BP006	BP056	BP030	BP036	BP029	BP053	BP005	13
							20P	SS17	16P	16P	SS18	20P		14
							BP065		BP035	BP034		BP062		15
							4P	20P	16P	16P	20P	4P		16
							BP004	BP052	BP028	BP055	BP027	BP051	BP003	17
							12P	20P	16P	16P	20P	12P		18
							BP020	BP050	BP026	BP025	BP049	BP019		19
							7P	12P	20P	20P	16P	7P		20
							BP012	BP040	BP048	BP057	BP059	BP010		21
							16P	20P	20P	16P				22
							BP038	BP046	BP045	BP037				23
							7P	12P	20P	12P	7P			24
							BP011	BP018	BP061	BP017	BP019			25
							4P	4P						26
							BP002	BP001						27

4P - 6 BURNABLE POISON ROD CLUSTER
 7P - 7 BURNABLE POISON ROD CLUSTER
 12P - 12 BURNABLE POISON ROD CLUSTER
 16P - 16 BURNABLE POISON ROD CLUSTER
 20P - 20 BURNABLE POISON ROD CLUSTER
 SSxx - SECONDARY SOURCE

Figure 1.3
NORTH ANNA UNIT 2 - CYCLE 8
MOVABLE DETECTOR LOCATIONS

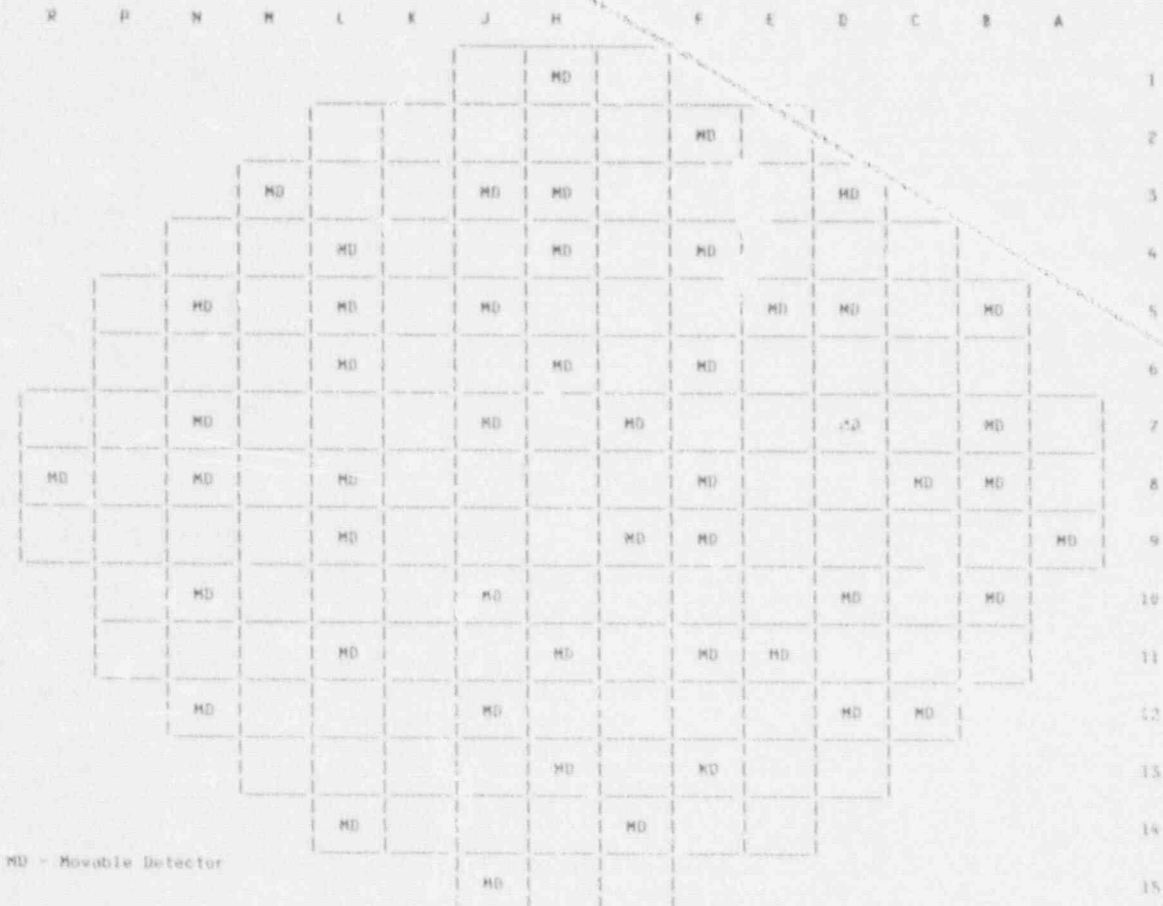
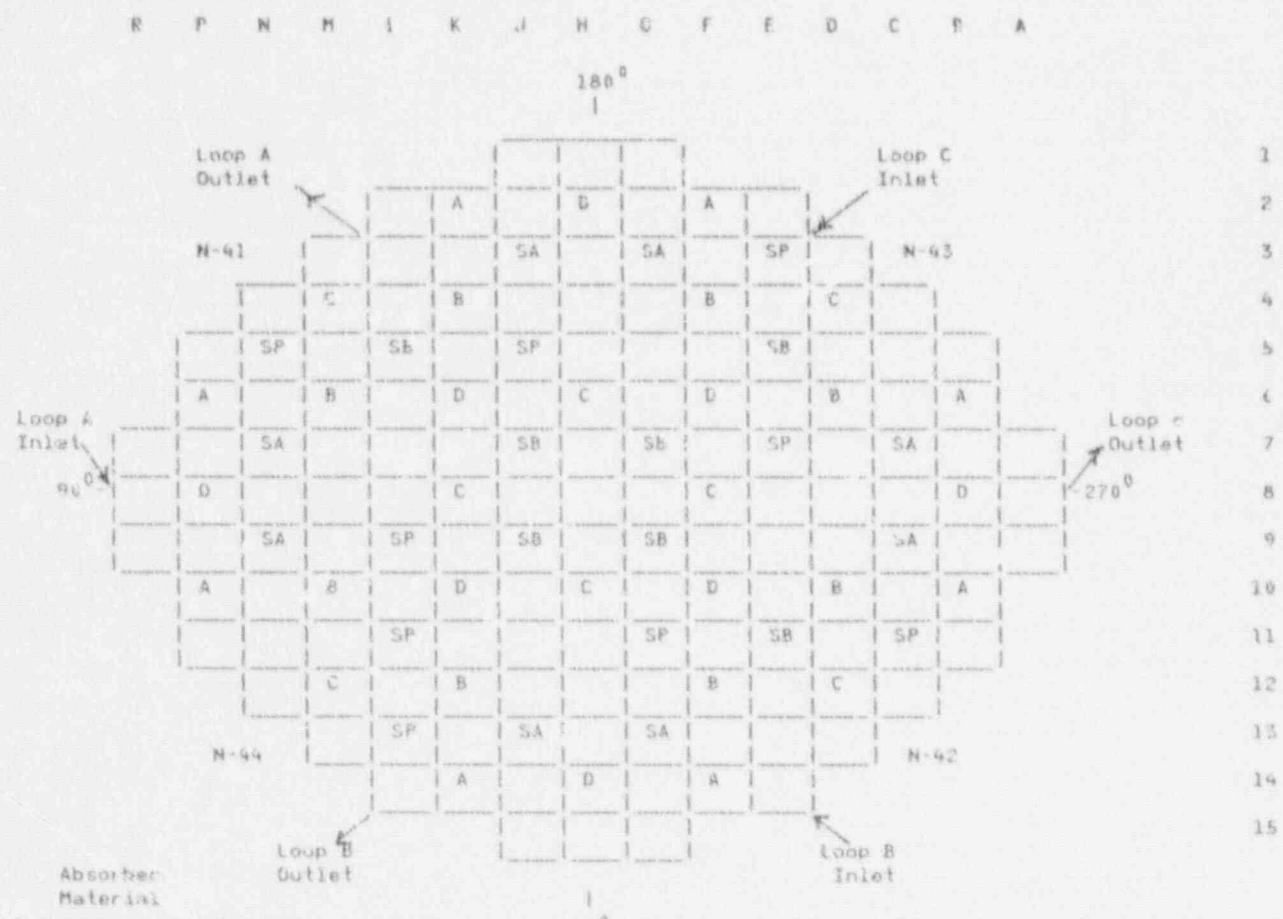


Figure 1.4
NORTH ANNA UNIT 2 - CYCLE 8
CONTROL ROD LOCATIONS



Function	Number of Clusters	CALLED NORTH
Control Bank D	8	
Control Bank C	8	
Control Bank B	8	
Control Bank A	8	
Shutdown Bank SB	8	
Shutdown Bank SA	8	
SP (Spare Rod Locations)	8	

Section 2

BURNUP

The burnup history for the North Anna Unit 2, Cycle 8 core is graphically depicted in Figure 2.1. The North Anna 2, Cycle 8 core achieved a burnup of 18,239 MWD/MTU. As shown in Figure 2.2, the average load factor for Cycle 8 was 95.2% when referenced to rated thermal power (2893 MW(t)). Unit 2 performed a power coastdown starting on January 14, 1992 until shutdown for refueling on February 26, 1992.

Radial (X-Y) burnup distribution maps show how the core burnup is shared among the various fuel assemblies, and thereby allow a detailed burnup distribution analysis. The NEWTOTE³ computer code is used to calculate these assemblywise burnups. Figure 2.3 is a radial burnup distribution map in which the assemblywise burnup accumulation of the core at the end of Cycle 8 operation is given. For comparison purposes, the design values are also given. Figure 2.4 is a radial burnup distribution map in which the percentage difference comparison of measured and predicted assemblywise burnup accumulation at the end of Cycle 8 operation is also given. As can be seen from this figure, the accumulated assembly burnups were generally within $\pm 2.98\%$ of the predicted values. In addition, deviation from quadrant symmetry in the core throughout the cycle was no greater than $\pm 6.30\%$.

The burnup sharing on a batch basis is monitored to verify that the core is operating as designed and to enable accurate end-of-cycle batch

burnup predictions to be made for use in reload fuel design studies. Batch definitions are given in Figure 1.1. As seen in Figures 2.5A, 2.5B, 2.5C, 2.5D, and 2.5E the batch burnup sharing for North Anna 2, Cycle 8 followed design predictions closely with no batch deviating from prediction by more than 1.69%. Symmetric burnup in conjunction with agreement between actual and predicted assemblywise burnups and batch burnup sharing indicate that the Cycle 8 core did deplete as designed.

Figure 2.1
NORTH ANNA UNIT 2 - CYCLE 8
CORE BURNUP HISTORY

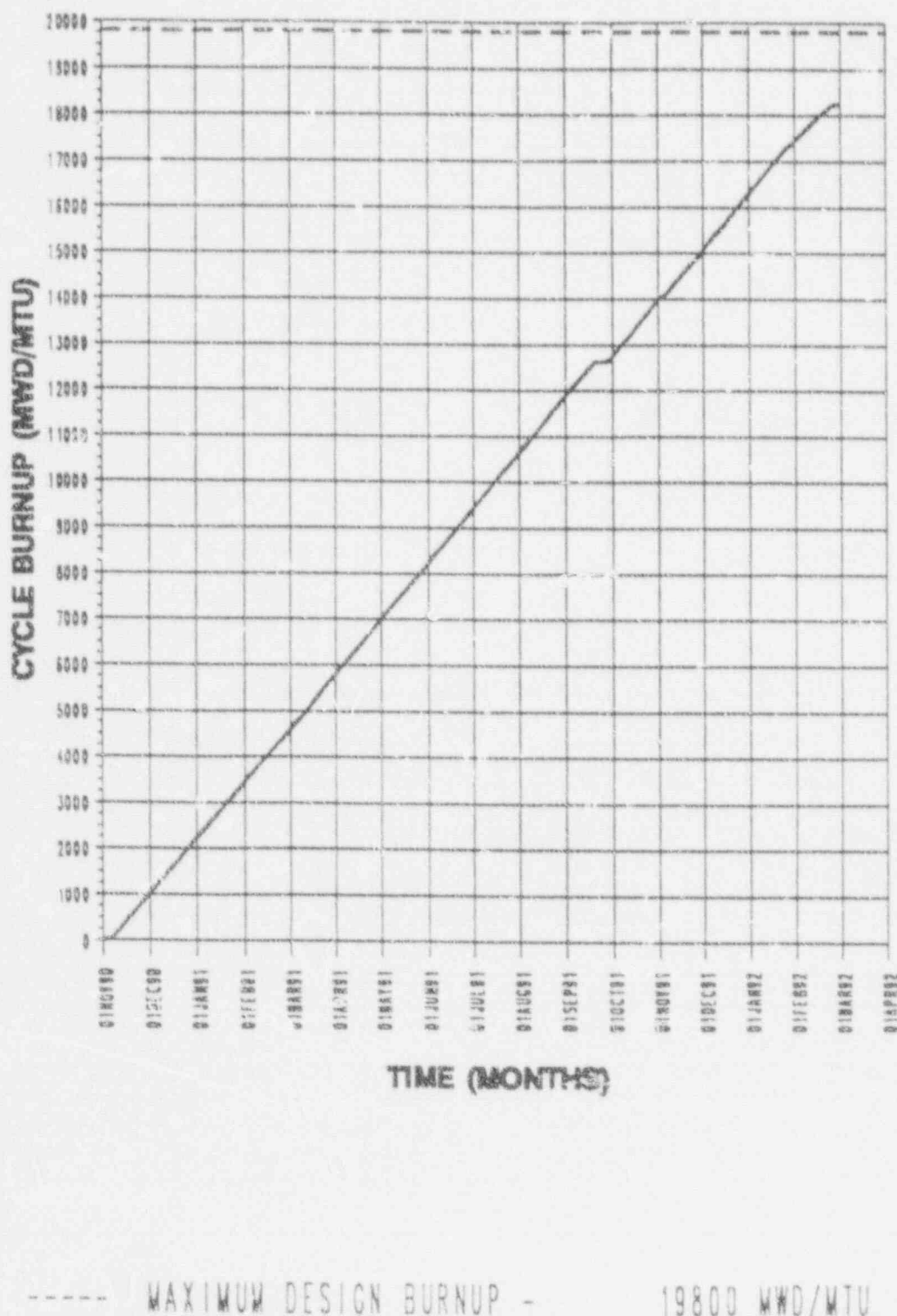


Figure 2.2
NORTH ANNA UNIT 2 - CYCLE 8
MONTHLY AVERAGE LOAD FACTORS

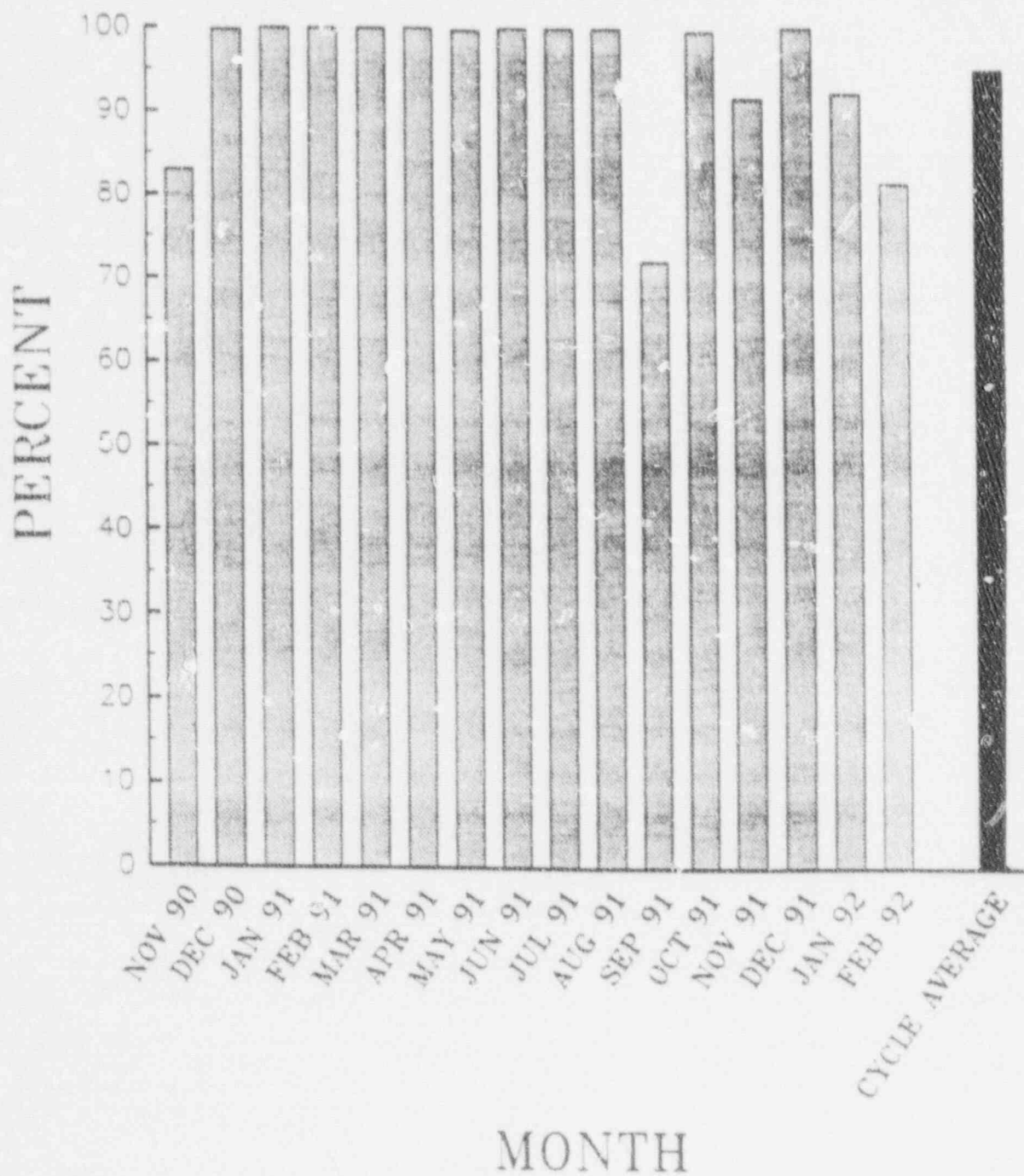


Figure 2.3
NORTH ANNA UNIT 2 - CYCLE 8
ASSEMBLYWISE ACCUMULATED BURNUP
MEASURED AND PREDICTED
(GWD/MTU)

Figure 2.4
NORTH ANNA UNIT 2 - CYCLE 8
ASSEMBLYWISE ACCUMULATED BURNUP
COMPARISON OF MEASURED AND PREDICTED
(GWD/MTU)

	R	P	H	H	L	S	J	H	G	F	E	B	C	B	A
1							39.13 41.84 39.30					MEASURED			
							8.51 0.09 0.75					B/P Z DIFF			
2							41.25 35.65 19.16 35.61 19.25 35.99 41.39								2
							-0.20 -0.05 0.97 -0.02 0.55 0.89 0.13								
3							46.98 19.74 22.22 39.39 23.87 39.69 22.99 20.20 45.90								3
							0.86 0.24 -1.71 -0.73 -4.57 0.02 1.67 2.59 2.92								
4							45.26 36.57 23.75 44.55 26.62 44.10 24.61 56.62 23.95 35.06 44.40								4
							1.45 -0.69 -0.02 -0.01 -0.56 -0.77 -0.40 -0.67 0.86 1.32 -0.47								
5							40.89 19.52 25.18 44.07 26.58 43.19 45.61 28.85 48.50 23.66 19.72 41.64								5
							-1.07 -1.95 -2.39 -1.10 -1.12 0.18 0.07 0.99 0.79 -0.15 -1.24 -0.10 0.26								
6							55.20 22.56 44.57 24.59 63.95 25.24 42.01 25.12 -5.51 < .30 44.14 22.29 35.62								6
							-1.53 -1.11 -0.80 -1.04 -1.59 1.68 0.54 1.19 -0.21 -1.65 -1.78 -1.42 -0.14								
7							39.10 19.15 39.27 29.13 42.61 24.17 44.47 25.28 44.66 25.10 42.84 23.59 38.86 18.86								7
							0.17 -0.09 -1.04 -2.21 -1.12 -2.17 -0.43 2.31 0.91 1.61 -0.58 -0.43 -2.08 -1.52 -0.95								
8							42.15 36.62 25.59 43.85 42.63 42.57 24.28 53.05 24.66 42.78 42.76 41.78 23.40 35.79 41.98								8
							0.78 2.79 -1.58 -1.28 -0.60 -0.71 -1.67 -0.32 -0.04 -0.22 -0.48 -2.34 -2.58 0.65 0.82								
9							39.09 18.96 38.50 29.23 42.21 24.45 44.63 26.13 45.11 26.64 43.42 24.36 39.69 19.20 38.75								9
							0.14 -1.51 -2.98 -1.83 -2.06 -1.01 -0.50 -2.35 1.01 -0.25 0.75 -1.30 -0.01 3.26 -0.74								
10							55.24 21.92 46.80 24.75 44.55 24.58 42.20 26.42 44.17 28.53 44.69 22.98 35.75								10
							-1.21 -3.05 -0.72 0.42 -0.65 -1.17 0.80 -2.65 -0.99 -0.48 -0.52 1.62 0.24								
11							41.28 19.26 23.90 44.66 24.28 43.06 42.50 42.52 26.62 44.38 24.19 20.14 41.67								11
							-0.13 0.30 0.51 0.23 -1.51 -0.54 -1.51 -2.00 -0.12 -0.59 1.84 2.24 0.57								
12							45.10 35.10 23.93 44.18 23.91 45.48 24.06 44.38 25.71 35.53 45.76								12
							1.15 1.41 0.80 -1.66 -3.22 -2.17 -2.64 -1.22 -0.11 2.67 2.57								
13							45.95 19.80 21.65 38.75 25.15 38.58 22.18 19.58 44.57						ARITHMETIC AVG	13	
							3.01 0.59 -4.35 -2.35 -3.36 -2.27 -1.92 -0.55 -0.07						EPCT DIFF = -0.42		
14							42.34 55.93 19.16 55.58 18.58 55.17 41.09								14
							2.45 0.75 0.08 -0.67 -2.93 -1.60 -0.59								
15							1 STANDARD DEV						AVG ABS PCF		15
							+ 0.95						DIFF X 1.12		

BATCH SHARING

THRD/HTR				
BATCH	NO. OF ASSEMBLIES	BOC BATCH BURNUP	EDC BATCH BURNUP	CYCLE BURNUP
N1/5	2	22,603	42,104	19,501
N1/6	1	37,921	45,097	7,176
N1/7	1	34,556	53,027	18,471
N1/10A	12	23,945	38,513	14,568
N1/10B	1	23,443	45,108	21,665
4	2	23,869	42,678	18,809
5A	8	33,607	38,916	5,309
7A	7	38,225	45,258	7,033
8A	8	34,997	41,407	6,410
8B	4	35,465	41,945	6,480
9A	16	23,632	44,219	20,587
9B	31	20,543	40,134	19,591
10A	28	0	23,953	23,953
10B	36	0	21,890	21,890
CYCLE AVERAGE ACCUMULATED BURNUP = 18,239				

BURNUP TILT

ZB 10 10 1 NE 10 0 732

Fig. 10. 35° N. = 0.00

Figure 2.5A
NORTH ANNA UNIT 2 - CYCLE 8
SUB-BATCH BURNUP SHARING

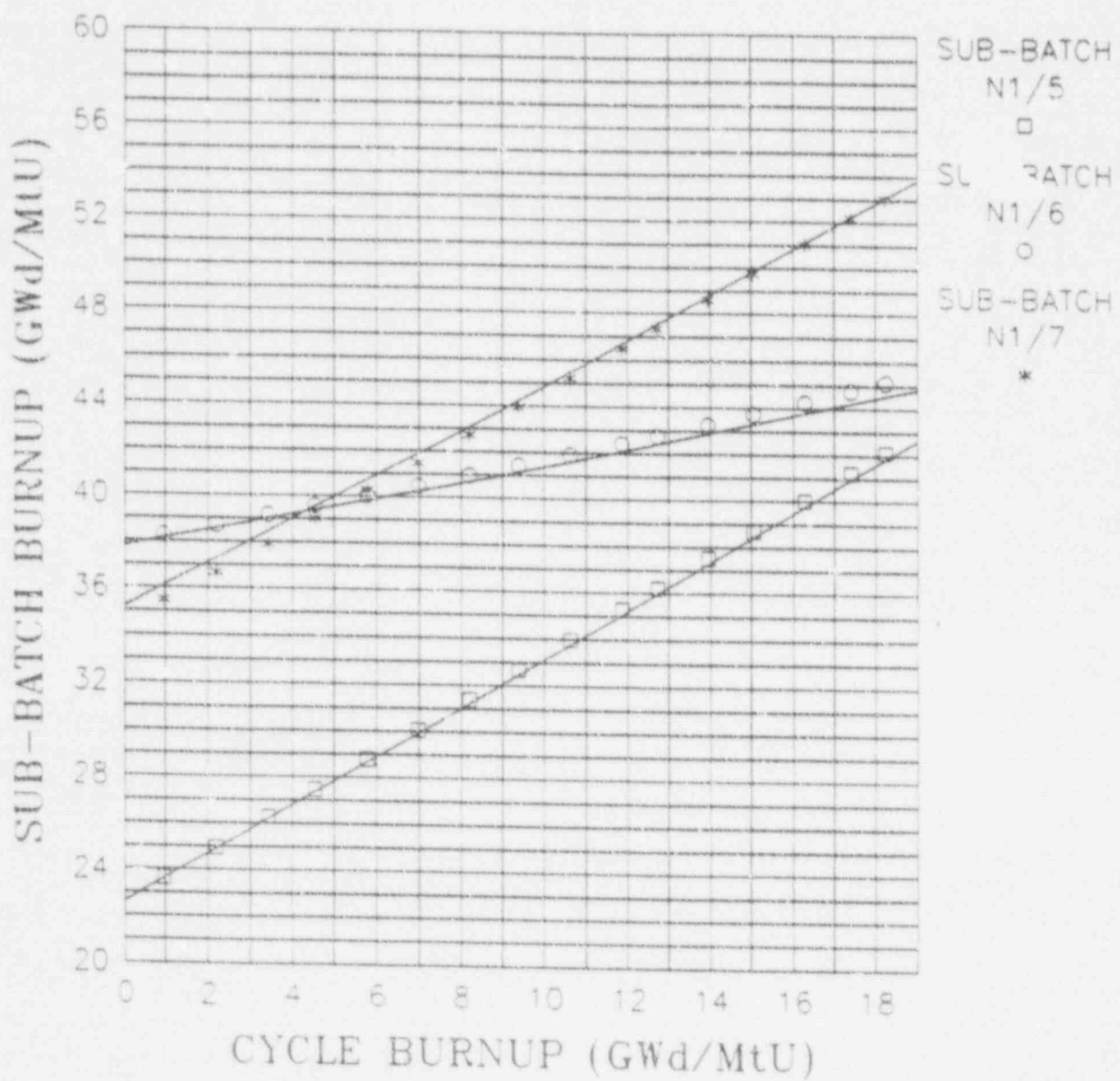


Figure 2.5B
NORTH ANNA UNIT 2 - CYCLE 8
SUB-BATCH BURNUP SHARING

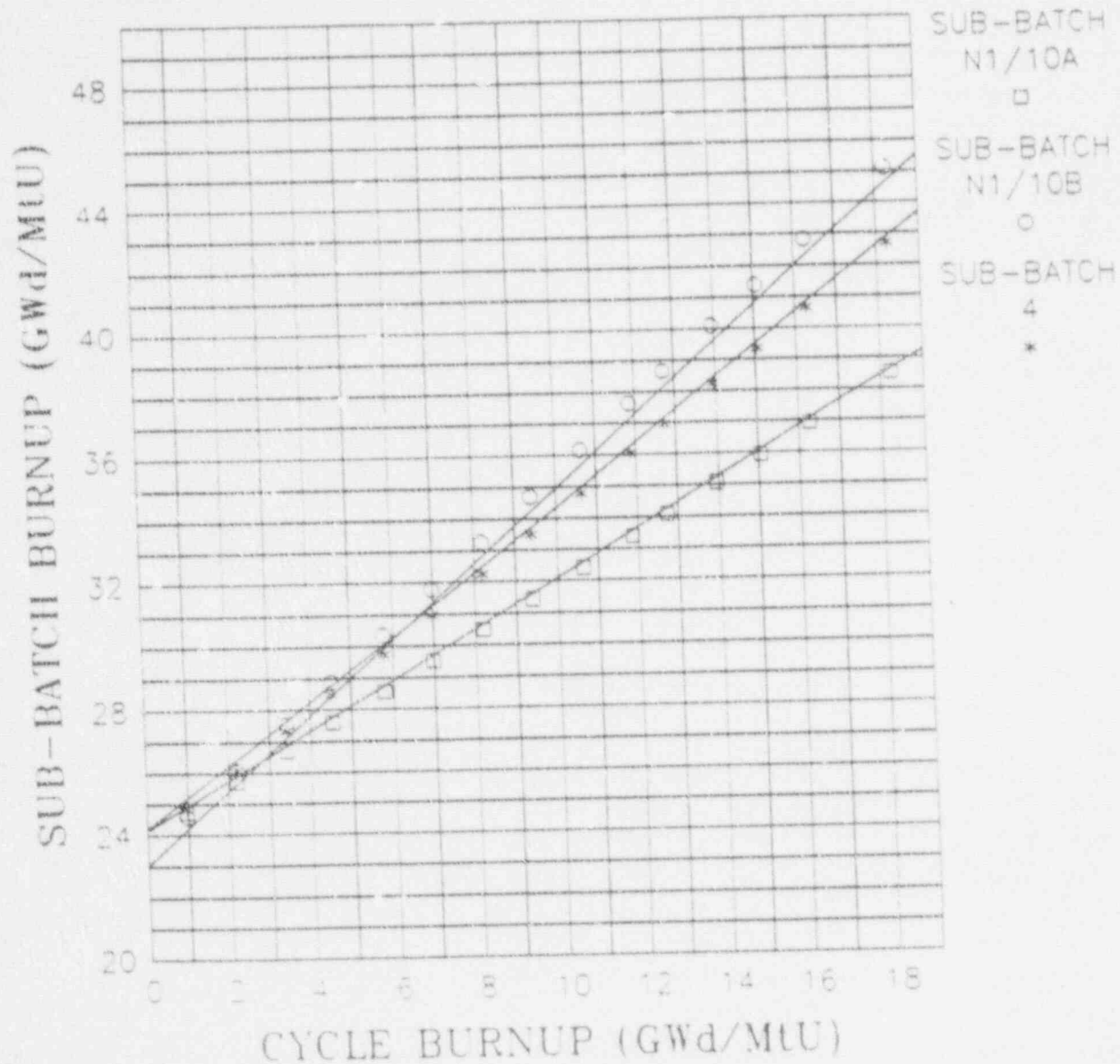


Figure 2.5C
NORTH ANNA UNIT 2 - CYCLE 8
SUB-BATCH BURNUP SHARING

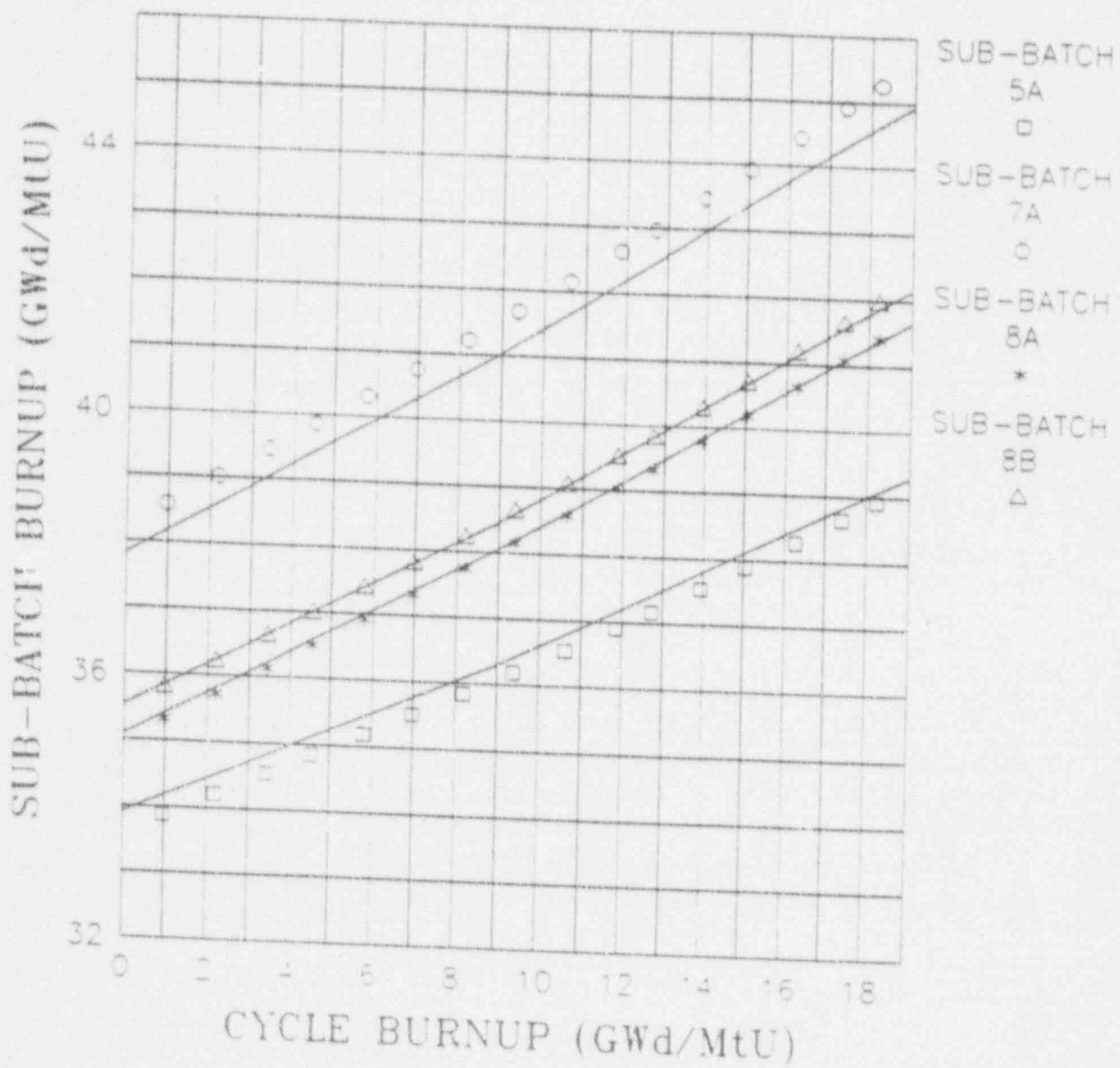


Figure 2.5D
NORTH ANNA UNIT 2 - CYCLE 8
SUB-BATCH BURNUP SHARING

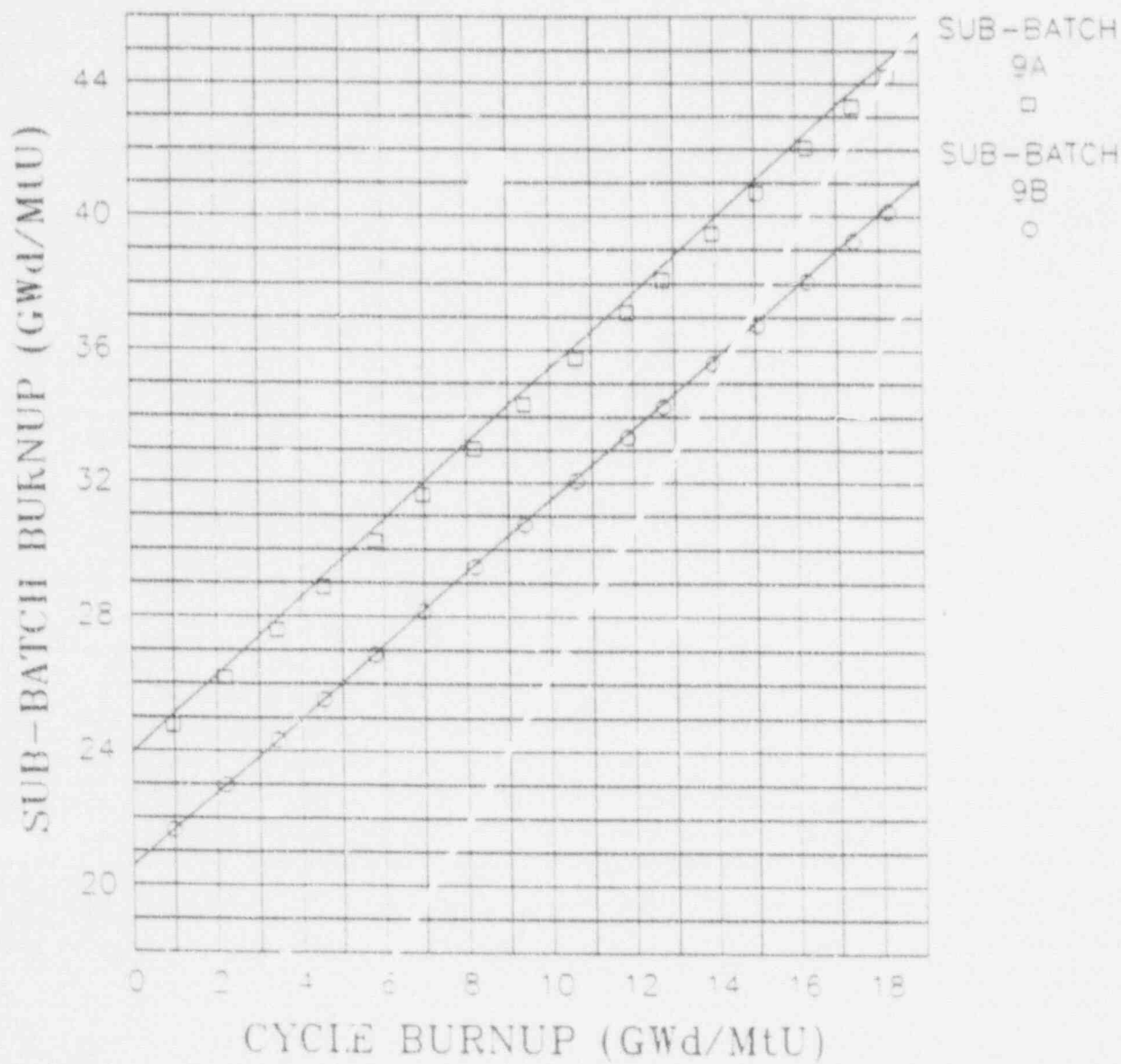
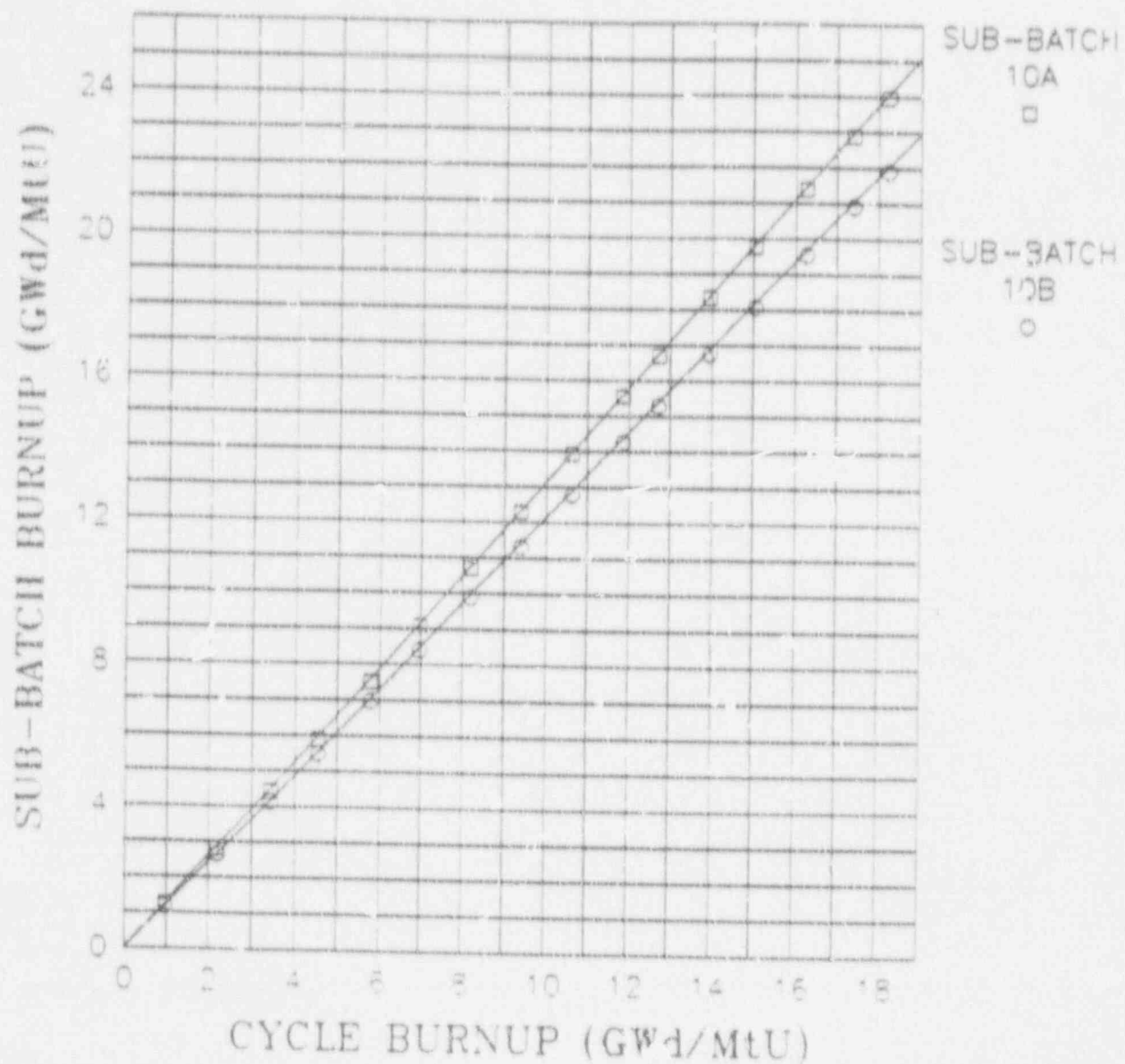


Figure 2.5E
NORTH ANNA UNIT 2 - CYCLE 8
SUB-BATCH BURNUP SHARING

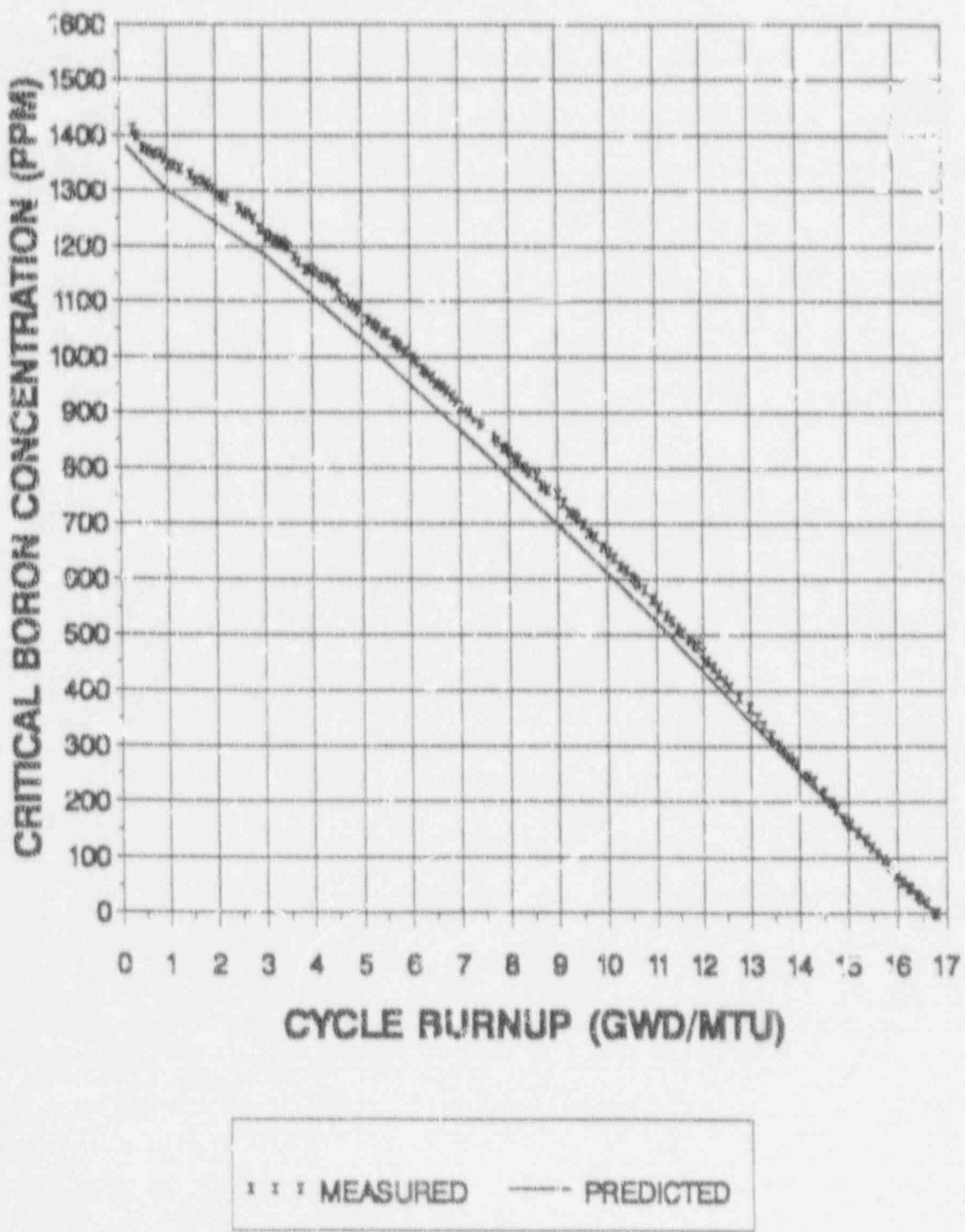


Section 3

REACTIVITY DEPLETION

The primary coolant critical boron concentration is monitored for the purposes of following core reactivity and to identify any anomalous reactivity behavior. The FOLLOW* computer code was used to normalize "actual" critical boron concentration measurements to design conditions taking into consideration control rod position, xenon concentration, moderator temperature, and power level. The normalized critical boron concentration versus burnup curve for the North Anna 2, Cycle 8 core is shown in Figure 3.1. It can be seen that the measured data typically compared to within 58 ppm of the design prediction. This corresponds to $\pm 0.39\% \Delta K/K$ which is within the $\pm 1\% \Delta K/K$ criterion for reactivity anomalies set forth in Section 4.1.1.1.2 of the Technical Specifications. In conclusion, the trend indicated by the critical boron concentration verifies that the Cycle 8 core depleted as expected without any reactivity anomalies.

Figure 3.1
NORTH ANNA UNIT 2 - CYCLE 8
CRITICAL BORON CONCENTRATION vs. BURNUP
(HFP, ARO)



Section 4

POWER DISTRIBUTION

Analysis of core power distribution data on a routine basis is necessary to verify that the hot channel factors are within the Technical Specifications limits and to ensure that the reactor is operating without any abnormal conditions which could cause an "uneven" burnup distribution. Three-dimensional core power distributions are determined from movable detector flux map measurements using the INCORE⁶ computer program. A summary of all full core flux maps taken since the completion of startup physics testing for North Anna 2, Cycle 8 is given in Table 4.1. Power distribution maps were generally taken at monthly intervals with additional maps taken as needed.

Radial (X-Y) core power distribution for a representative series of incore flux maps are given in Figures 4.1, 4.2, and 4.3. Figure 4.1 shows a power distribution map that was taken early in cycle life. Figure 4.2 shows a power distribution map that was taken near mid-cycle burnup. Figure 4.3 shows a map that was taken near the end of cycle 8. The measured relative assembly powers were generally within 7.0% and the maximum average percent difference was equal to 2.5%. In addition, as indicated by the INCORE tilt factors, the power distributions were essentially symmetric for each case.

An important aspect of core power distribution follow is the monitoring of nuclear hot channel factors. Verification that these factors are

within Technical Specifications limits ensures that linear power density and critical heat flux limits will not be violated, thereby providing adequate thermal margin and maintaining fuel cladding integrity. North Anna Unit 2 Technical Specification 3.2.2 limited the axially dependent heat flux hot channel factor, $F_Q(Z)$, to $2.19 \times K(Z)$, where $K(Z)$ is the hot channel factor normalized operating envelope, and 2.19 is the F_Q limit at rated thermal power, both as specified in the Core Operations Limit Report (COLR).⁶ Figure 4.4 is a plot of the $K(Z)$ curve associated with the 2.19 $F_Q(Z)$ limit.

The axially dependent heat flux hot channel factors, $F_Q(Z)$, for a representative set of flux maps are given in Figures 4.5, 4.6, and 4.7. Throughout Cycle 8, the measured values of $F_Q(Z)$ were within the Technical Specifications limit. A summary of the maximum values of axially-dependent heat flux hot channel factors measured during Cycle 8 is given in Figure 4.8. This figure indicates that the minimum margin to the F_Q limit in the axial region covered by the Technical Specification 4.2.2.2 is 11.4%. (Technical Specification 4.2.2.2.g states that F_Q surveillance is not applicable in the lower core region from 0% to 15% inclusive, and the upper core region from 85% to 100% inclusive.)

Figure 4.9 shows the maximum values for the heat flux hot channel factor measured during Cycle 8. As can be seen from the figure, there was an approximate 16.00% margin from the maximum $F_Q(Z)$ to the 2.19 limit at the beginning of the cycle, which was the minimum margin seen for the cycle.

The value of the enthalpy rise hot channel factor, $F\delta H$, which is the ratio of the integral of the power along the rod with the highest integrated power to that of the average rod, is routinely followed. The Technical Specifications limit for this parameter is set such that the departure from nucleate boiling ratio (DNBR) limit will not be violated. Additionally, the $F\delta H$ limit ensures that the value of this parameter used in the LOCA+ECCS analysis is not exceeded during normal operation.

beginning of Cycle 8. Delta flux values decreased steadily to -5.3% near a cycle burnup of 14,300 MWD/MTU, where it then gradually increased to +3.6% before the coastdown. At the end of Cycle 8, the target delta flux increased to +4.2% due to the coastdown. This axial power shift can also be observed in the corresponding core average axial power distribution for a representative series of maps given in Figures 4.12 through 4.14. In Map N2-8-07 (Figure 4.12), taken at 1505 MWD/MTU, the axial power distribution had a shape peaked toward the middle of the core with a peaking factor of 1.208. In Map N2-8-14 (Figure 4.13), taken at approximately 9129 MWD/MTU, the axial power distribution peaked slightly toward the bottom of the core with an axial peaking factor of 1.157. Finally, in Map N2-8-25 (Figure 4.14), taken at 16,640 MWD/MTU, the axial peaking factor was 1.157, with the axial power distribution shifted slightly back toward the top. The history of F-Z during the cycle can be seen more clearly in a plot of F-Z versus burnup given in Figure 4.15.

In conclusion, the North Anna 2, Cycle 8 core performed satisfactorily with power distribution analyses verifying that design predictions were accurate and that the values of the $F_Q(Z)$ and $F\text{-delta-H}$ hot channel factors were within the limits of the Technical Specifications.

Table 4.1
NORTH ANNA UNIT 2 - CYCLE 8
SUMMARY OF FLUX MAPS FOR ROUTINE OPERATION

SI (MAP)	BURN ID	DATE	MWD/ RTD	BANK	F-Q(T) HOT CHANNEL FACTOR	F-DH(X) HOT CHAN. FACTOR	CORE F(Z) MAX	CORE MAX	CORE MAX LOG	AXIAL NO.					
					ASSY/PIN(AXIAL)	ASSY/PIN (F-Q(T))	ASSY/PIN (F-DH(X))	POINT							
					I	I	I	I							
17	112-14-91	1505	100	228	I01	IPI 57	I 3.874	B01	IPI 1.419	56	11.208	1.42811.0061	NE	-2.0081	46
18	101-09-91	2554	100	228	I01	IPI 57	I 3.861	B07	IJ 1.453	56	11.191	1.46111.0061	NE	-2.5161	46
19	102-12-91	3694	100	228	I01	IPI 57	I 3.859	B07	IJ 1.465	57	11.171	1.46811.0061	NE	-2.4691	46
110	103-02-91	4592	100	228	I01	IPI 58	I 3.872	B07	IJ 1.467	58	11.166	1.46711.0071	NE	-3.0621	46
111	104-03-91	5680	100	228	I01	FPI 59	I 3.806	B07	IJ 1.456	65	11.156	1.45111.0081	NE	-3.5581	46
112	104-23-91	6673	100	228	I05	IPI 67	I 3.826	B07	IJ 1.459	96	11.157	1.45611.0071	NE	-3.0071	46
113	105-23-91	7854	100	228	I05	IPI 67	I 3.855	B07	IJ 1.457	87	11.160	1.45511.0071	NE	-4.6211	46
114	106-26-91	9129	100	228	I05	IPI 68	I 3.831	B07	IJ 1.458	48	11.157	1.45911.0071	NE	-6.5321	46
115	107-17-91	10946	100	228	I05	IPI 68	I 3.854	B07	IJ 1.453	48	11.156	1.45611.0071	NE	-6.5361	46
116	108-13-91	11118	100	228	I07	I21 53	I 3.855	B07	IJ 1.451	48	11.156	1.45811.0071	NE	-6.2621	46
117	109-13-91	12356	100	228	I07	I21 54	I 3.835	B07	IJ 1.452	53	11.158	1.45111.0061	NE	-6.5621	46
118	109-28-91	12669	100	151	I06	I21 29	I 4.870	B04	H1 1.465	54	11.177	1.46711.0151	NE	-5.7701	46
119	110-01-91	12753	100	228	I07	I21 53	I 3.855	F07	FR 1.439	52	11.171	1.46811.0061	NE	-5.2091	46
120	110-15-91	13286	100	228	I07	I21 54	I 3.855	B07	IJ 1.455	55	11.172	1.44511.0061	NE	-5.0861	46
123	111-12-91	14582	100	228	I07	I21 53	I 3.865	B07	IJ 1.428	53	11.179	1.43611.0061	NE	-5.2821	46
124	112-12-91	15692	100	228	I07	I21 54	I 3.868	B07	FR 1.422	53	11.171	1.43111.0061	NE	-6.6191	46
125	101-08-91	16648	100	228	I07	I21 54	I 3.837	F07	FR 1.426	53	11.157	1.43911.0021	NE	-5.5751	46
126	102-10-91	17259	100	228	I07	I21 52	I 3.805	J06	EF 1.405	17	11.166	1.43111.0021	NE	-6.2231	46

NOTES: HOT SPOT LOCATIONS ARE SPECIFIED BY GIVING ASSEMBLY LOCATIONS (E.G., H-8 IS THE CENTER-OF-CORE ASSEMBLY), FOLLOWED BY THE PIN LOCATION (DENOTED BY THE "Y" COORDINATE WITH THE SEVENTEEN ROWS OF FUEL RODS LETTERED A THROUGH P AND THE "X" COORDINATE DESIGNATED IN A SIMILAR MANNER). IN THE "Z" DIRECTION THE CORE IS DIVIDED INTO 61 AXIAL POINTS STARTING FROM THE TOP OF THE CORE.

1. F-Q(T) INCLUDES A TOTAL UNCERTAINTY OF 1.05×1.05 .

2. CORE TILT - DEFINED AS THE AXIAL QUADRANT POWER TILT FROM INCORE.

3. MAPS 21 and 22 WERE QUARTER-CORE FLUX MAPS TAKEN FOR INCORE/EXCORE CALIBRATION, LIVE CALIBRATION.

Figure 4.1
NORTH ANNA UNIT 2 - CYCLE 8
ASSEMBLYWISE POWER DISTRIBUTION N2-8-07

R	D	H	I	K	J	H	G	F	I	D	C	B	K		
PREDICTED		0.26	0.37	0.26						PREDICTED					
MEASURED		0.26	0.34	0.26						MEASURED					
PCT DIFFERENCE		-5.5	-5.5	-6.2						PCT DIFFERENCE					
		0.35	0.62	1.09	0.95	1.09	0.67	0.35							
		0.36	0.66	1.11	0.96	1.11	0.66	0.36							
		4.5	7.6	3.8	1.8	2.1	5.2	3.3							
		0.35	1.10	1.25	1.20	1.30	1.20	1.25	1.10	0.35					
		0.35	1.10	1.25	1.21	1.31	1.21	1.26	1.12	0.36					
		1.8	6.5	0.6	1.1	0.9	3.2	2.7	2.6	3.6					
		0.35	0.66	1.29	1.16	1.57	1.16	1.32	1.16	1.29	0.66	0.35			
		0.36	0.66	1.30	1.16	1.56	1.15	1.33	1.17	1.30	0.66	0.36			
		3.0	6.6	0.5	0.6	1.4	1.4	0.7	1.1	0.6	0.1	0.6			
		0.35	1.10	1.29	1.16	1.29	1.19	1.12	1.19	1.29	1.10	0.35			
		0.32	1.07	1.27	1.16	1.29	1.25	1.15	1.27	1.31	1.15	1.27	0.36		
		2.3	7.3	1.5	1.2	0.5	2.8	2.9	2.2	1.1	-0.1	1.7	2.8		
		0.67	1.25	1.16	1.29	1.16	1.32	1.06	1.32	1.18	1.29	1.16	1.25	0.67	
		0.67	1.24	1.15	1.29	1.16	1.36	1.07	1.35	1.19	1.28	1.15	1.23	0.65	
		0.9	6.9	0.6	0.8	0.5	2.9	2.9	2.5	1.3	-1.3	2.2	0.5	0.7	
		0.26	1.09	1.20	1.32	1.19	1.31	1.19	1.30	1.19	1.51	1.19	1.32	0.26	
		0.27	1.09	1.18	1.30	1.17	1.29	1.25	1.35	1.21	1.53	1.18	1.27	0.26	
		3.1	9.0	1.3	1.3	1.1	3.8	5.6	2.2	1.6	-0.2	3.6	2.3	0.7	
		0.32	0.93	1.30	1.15	1.10	1.00	1.30	0.95	1.30	1.00	1.10	1.15	0.32	
		0.33	0.93	1.28	1.15	1.10	1.00	1.29	0.97	1.30	1.01	1.09	1.09	0.33	
		3.1	8.0	1.6	0.8	0.0	0.0	0.5	2.0	0.1	0.2	1.1	3.6	2.3	0.6
		0.26	1.09	1.20	1.37	1.19	1.51	1.19	1.30	1.19	1.51	1.19	1.32	0.26	
		0.27	1.07	1.16	1.29	1.19	1.50	1.17	1.29	1.19	1.51	1.19	1.30	0.27	
		3.1	7.3	3.4	1.7	0.1	0.5	1.1	1.1	0.0	0.1	0.2	1.4	0.5	1.8
		0.62	1.25	1.16	1.29	1.18	1.3	1.06	1.32	1.18	1.29	1.16	1.25	0.62	
		0.60	1.21	1.15	1.30	1.18	1.32	1.05	1.31	1.17	1.29	1.17	1.27	0.60	
		5.3	3.5	0.7	0.7	0.1	0.5	0.2	1.0	0.8	0.6	3.6	1.1	2.8	
		0.35	1.10	1.29	1.15	1.29	1.19	1.12	1.19	1.29	1.16	1.29	1.10	0.35	
		0.32	1.09	1.29	1.16	1.28	1.18	1.11	1.19	1.29	1.15	1.31	1.12	0.34	
		0.5	0.5	0.0	1.0	0.8	0.8	0.7	0.5	0.5	0.2	1.5	1.7	2.8	
		0.27	0.86	1.29	1.16	1.32	1.14	1.32	1.16	1.29	0.86	0.56			
		0.6	0.85	1.30	1.15	1.50	1.12	1.30	1.15	1.29	0.86	0.56			
		1.9	1.2	3.0	0.7	1.4	1.8	1.8	1.6	0.7	0.8	1.8	2.5		
		0.35	1.10	1.25	1.25	1.20	1.50	1.20	1.25	1.15	0.35				
		0.36	1.11	1.25	1.17	1.28	1.18	1.24	1.09	1.09	0.36				
		2.4	1.0	2.2	2.6	1.8	1.8	1.6	1.2	0.7	2.1				
		0.35	0.67	1.09	0.95	1.09	0.67	0.67	0.67	0.67	0.35				
		0.36	0.65	1.10	0.93	1.07	0.65	0.62	0.62	0.52					
		6.5	6.5	1.0	0.8	1.5	1.1	1.1	1.8						
STANDARD DEVIATION		0.26	0.32	0.26						AVERAGE					
V-1.126		0.26	0.33	0.26						PCT DIFFERENCE					
		6.5	2.1	0.9						= 1.8					

第二輯

標號：NO. : N2-8-07

DATE: 12/16/90

POWER = 100%

CONTROL ROD POSITION

E-B(7) - 3-876

OPTIM

A BANK AT 220 STEPS

$F = \text{DM}(\mu) \approx 1.61\%$

NW 1 0035 INC 1 0093

E373 - 3 1.208

SF 0-9970

F(XY) = 0.142

BURNUP # 1505

A.9. $\approx -2.005\%$

Figure 4.2
NORTH ANNA UNIT 2 - CYCLE 8
ASSEMBLYWISE POWER DISTRIBUTION N2-8-14

B	P	H	M	L	K	J	H	G	F	E	D	C	B	A		
PREDICTED		0.28	0.34	0.28												
MEASURED		0.29	0.35	0.28												
PCT. DIFFERENCE		3.5	3.5	3.5												
		0.54	0.61	1.02	0.89	1.02	0.61	0.54								
		0.56	0.62	1.03	0.89	1.03	0.63	0.55								
		4.5	6.9	0.3	0.2	1.0	3.1	3.7								
		6.37	1.07	1.75	1.13	1.31	1.15	1.25	1.07	0.87						
		0.37	1.07	1.21	1.15	1.50	1.19	1.26	1.10	0.39						
		0.8	0.6	-1.5	-0.5	-0.7	-0.6	2.2	3.0	4.6						
		0.37	0.85	1.30	1.15	1.56	1.11	1.56	1.15	1.50	0.85	0.57				
		0.58	0.85	1.31	1.17	1.56	1.11	1.56	1.16	1.52	0.86	0.58				
		1.2	0.0	0.5	-0.7	-0.1	-0.1	-0.3	1.5	1.7	1.2	1.9				
		0.56	1.07	1.50	1.13	1.37	1.17	1.10	1.17	1.37	1.15	1.30	1.07	0.54		
		0.53	1.05	1.28	1.17	1.56	1.19	1.11	1.19	1.59	1.16	1.29	1.07	0.55		
		1.9	-1.9	-1.6	1.5	-0.9	1.6	1.8	1.6	1.8	0.5	-0.6	0.6	3.5		
		0.61	1.25	1.13	1.37	1.17	1.37	1.06	1.37	1.17	1.37	1.13	1.25	0.61		
		0.61	1.22	1.17	1.36	1.17	1.60	1.08	1.60	1.19	1.56	1.11	1.22	0.63		
		-0.6	-0.6	-0.6	-0.7	-0.9	1.8	1.9	2.0	1.5	-0.7	-1.6	-0.5	7.1		
		0.28	1.02	1.13	1.56	1.17	1.37	1.19	1.37	1.19	1.37	1.17	1.36	1.13	1.02	0.28
		0.28	1.03	1.12	1.56	1.15	1.56	1.22	1.91	1.21	1.60	1.17	1.31	1.11	1.02	0.28
		3.5	0.2	-1.3	-1.6	-1.6	2.5	2.5	2.2	2.0	0.1	-3.6	-1.6	-0.8	0.6	
		0.56	0.89	1.31	1.11	1.09	1.05	1.37	1.00	1.37	1.03	1.89	1.11	1.51	0.89	0.59
		0.55	0.89	1.29	1.10	1.08	1.05	1.36	1.02	1.36	1.04	1.88	1.07	1.29	0.89	0.58
		3.5	0.2	-1.6	-1.0	-0.5	-0.6	-1.0	2.6	0.6	0.6	-0.7	-3.6	-1.7	-0.9	1.8
		0.28	1.02	1.13	1.56	1.17	1.37	1.19	1.37	1.19	1.37	1.17	1.36	1.13	1.02	0.28
		0.28	1.01	1.10	1.54	1.16	1.56	1.17	1.35	1.20	1.37	1.18	1.35	1.13	1.03	0.28
		3.5	-0.9	-5.1	-1.7	-0.8	-0.8	-1.7	-1.7	0.6	0.6	1.0	-0.9	-0.1	1.0	-0.5
		0.61	1.03	1.13	1.37	1.17	1.37	1.06	1.37	1.17	1.37	1.13	1.25	0.61		
		0.60	1.07	1.12	1.58	1.17	1.38	1.05	1.36	1.17	1.38	1.15	1.26	0.65		10
		2.5	-2.5	-0.5	0.9	0.0	-1.0	-1.0	-1.2	-0.2	0.6	2.7	2.1	3.8		
		0.56	1.07	1.50	1.13	1.37	1.17	1.10	1.17	1.37	1.15	1.50	1.07	0.56		
		0.59	1.08	1.52	1.15	1.35	1.15	1.08	1.16	1.37	1.15	1.50	1.10	0.58		11
		0.7	0.8	1.0	1.6	-1.6	-2.0	-1.9	-1.1	0.2	1.1	-2.7	2.7	3.5		
		0.37	0.85	1.30	1.13	1.36	1.13	1.36	1.13	1.30	0.85	0.57				
		0.39	0.87	1.32	1.11	1.32	1.08	1.33	1.12	1.30	0.87	0.58				12
		9.1	2.8	1.6	-1.6	-3.0	-2.9	-2.1	-0.5	0.2	3.0	3.5				
		0.57	1.07	1.23	1.13	1.31	1.13	1.23	1.07	0.57						
		0.39	1.08	1.18	1.08	1.27	1.10	1.20	1.07	0.58						13
		6.1	1.6	-6.2	-4.2	-5.5	-2.7	-2.0	0.1	3.2						
		0.58	0.61	1.02	0.89	1.02	0.61	0.58								
		0.55	0.64	1.02	0.88	1.00	0.60	0.55								14
		3.7	3.7	0.1	-0.9	-2.6	-2.0	-2.1	-2.1							
		0.57	1.07	1.23	1.13	1.31	1.13	1.23	1.07	0.57						
		0.39	1.08	1.18	1.08	1.27	1.10	1.20	1.07	0.58						
		6.1	1.6	-6.2	-4.2	-5.5	-2.7	-2.0	0.1	3.2						
		0.58	0.61	1.02	0.89	1.02	0.61	0.58								
		0.55	0.64	1.02	0.88	1.00	0.60	0.55								
		3.7	3.7	0.1	-0.9	-2.6	-2.0	-2.1	-2.1							
STANDARD DEVIATION		0.28	0.34	0.28												
DEVIATION		0.29	0.35	0.27												15
+1.172		3.7	1.0	-1.6												

SUMMARY

MAP NO: N2-8-14 DATE: 06/24/91 POWER: 100%

CONTROL ROD POSITION: F-Q(T) = 1.831 Q(FR):

D BANK AT 228 STEPS F-DH(M) = 1.458 NW 0.9990 | NE 1.0068

F(Z) = 1.157 SW 0.9939 | SE 1.0002

F(XY) = 1.659

BURNUP = 9129 MWD/MTU A.O. = -4.532%

Figure 4.3
NORTH ANNA UNIT 2 - CYCLE 8
ASSEMBLYWISE POWER DISTRIBUTION N2-8-25

SUMMARY

MAP NO: N2-8-25

DATE: 01/10/92

POWER: 300%

CONTROL ROD POSITION

$$F(9(1)) = 3.837$$

- OPTR -

D SANK AT 228 STEPS

$$F = DH(M) \approx 1,424$$

NW 0.9933 | NE 1.0050

$$F(Z) = 1.157$$

SW 0.996 SE 0.9996

$$F(XY) = 1.439$$

BURNUP = 16640

A.G. = 3.57%

Figure 4.4
NORTH ANNA Unit 2 - CYCLE 8
HOT CHANNEL FACTOR NORMALIZED
OPERATING ENVELOPE

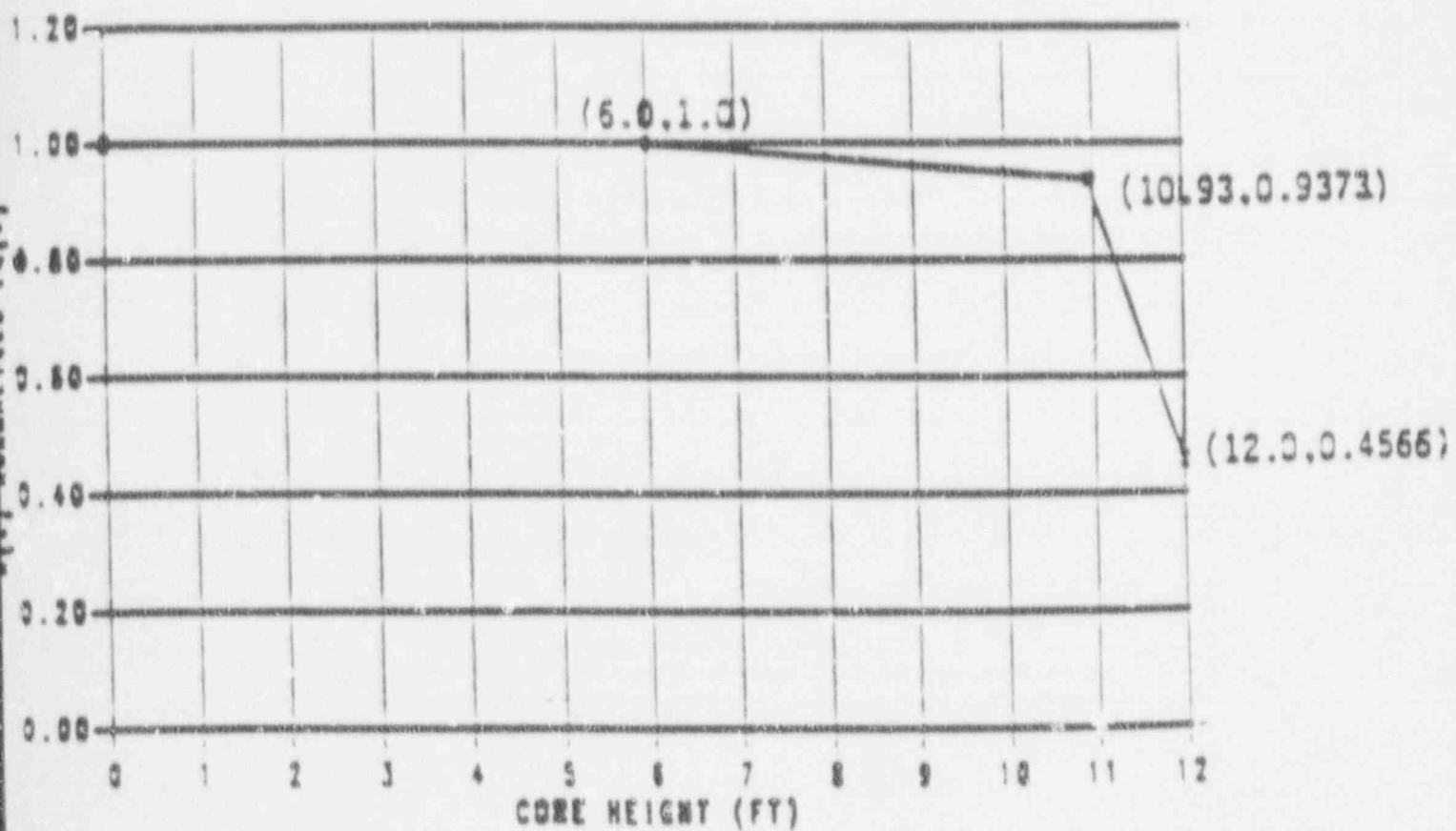


Figure 4.5
NORTH ANNA Unit 2 - CYCLE 8
HEAT FLUX HOT CHANNEL FACTOR, $F_Q(Z)$
N2-8-07

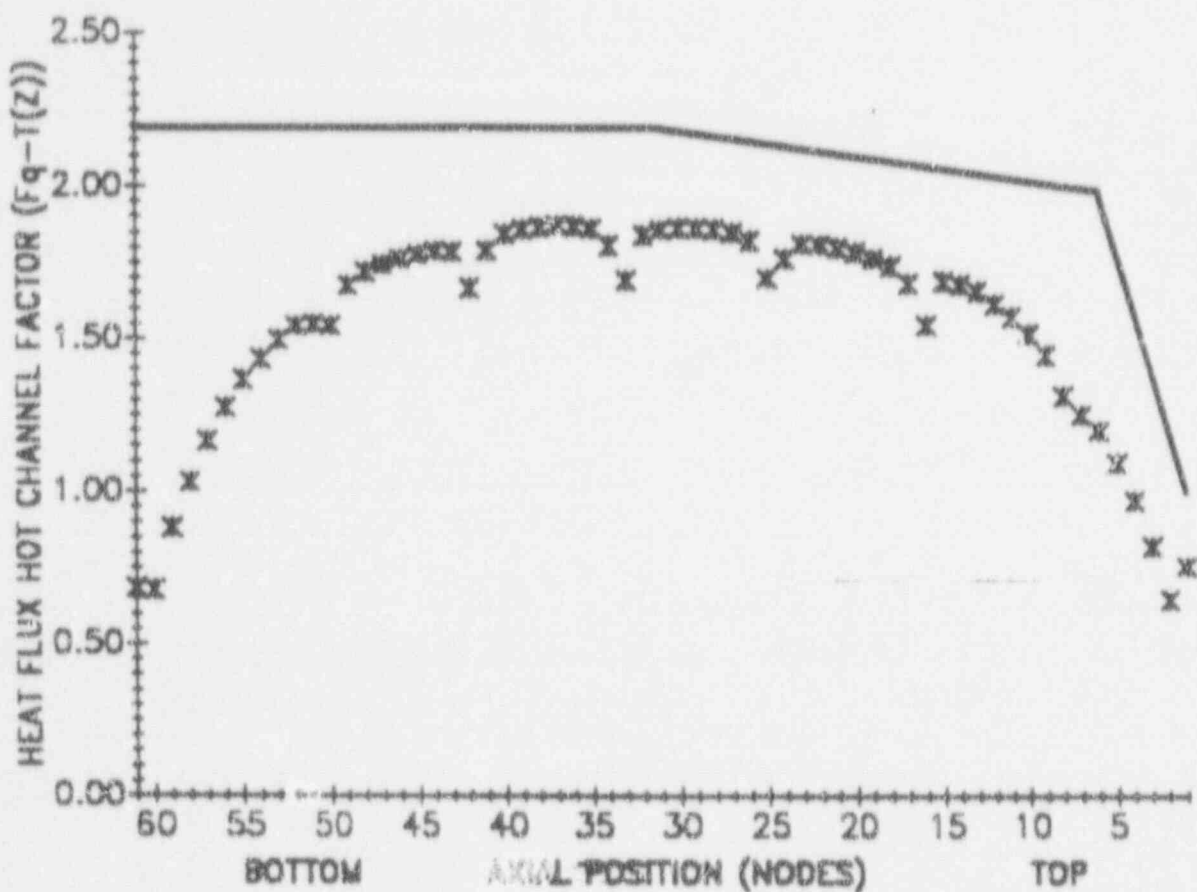


Figure 4.6
NORTH ANNA Unit 2 - CYCLE 8
HEAT FLUX HOT CHANNEL FACTOR, $F_Q(z)$
N2-8-14

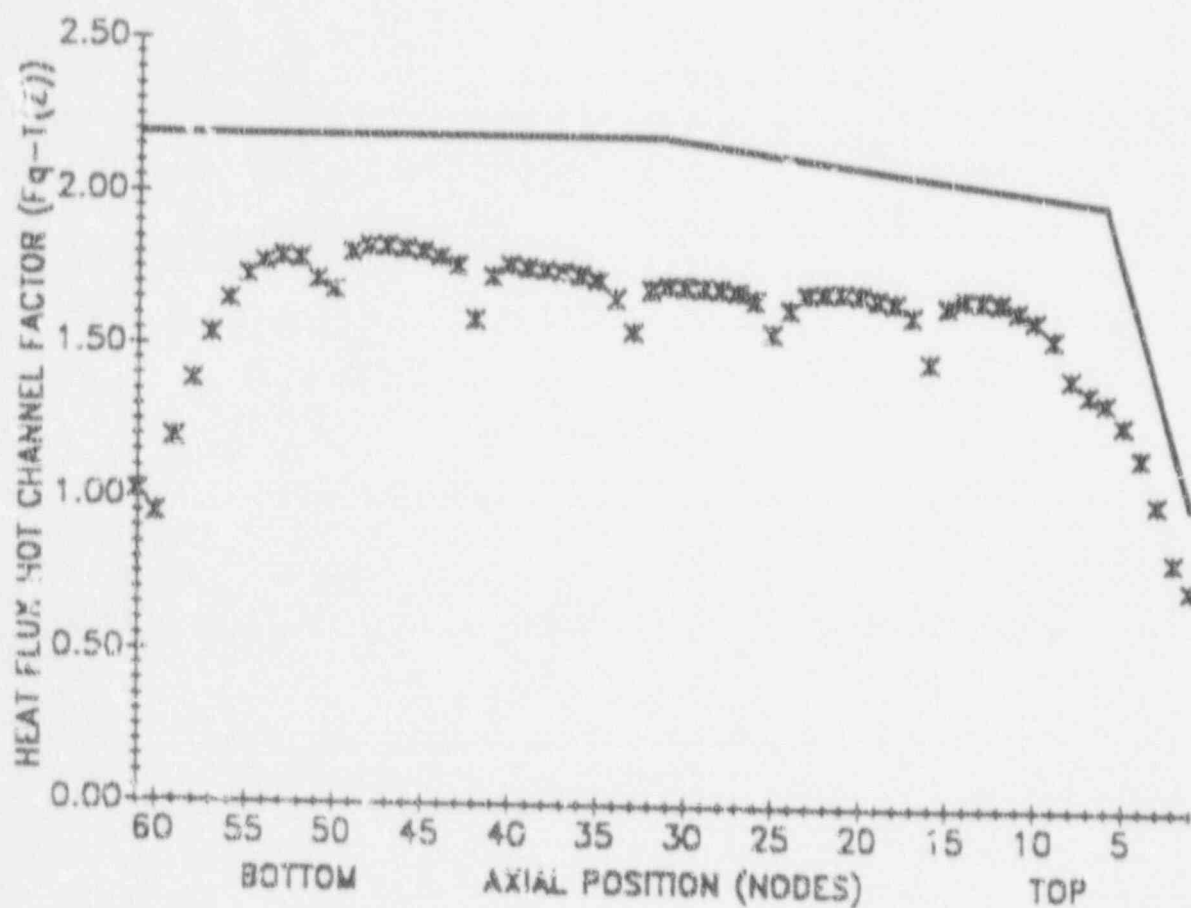


Figure 4.7
NORTH ANNA Unit 2 - CYCLE 8
HEAT FLUX HOT CHANNEL FACTOR, $F_Q(Z)$
N2-8-25

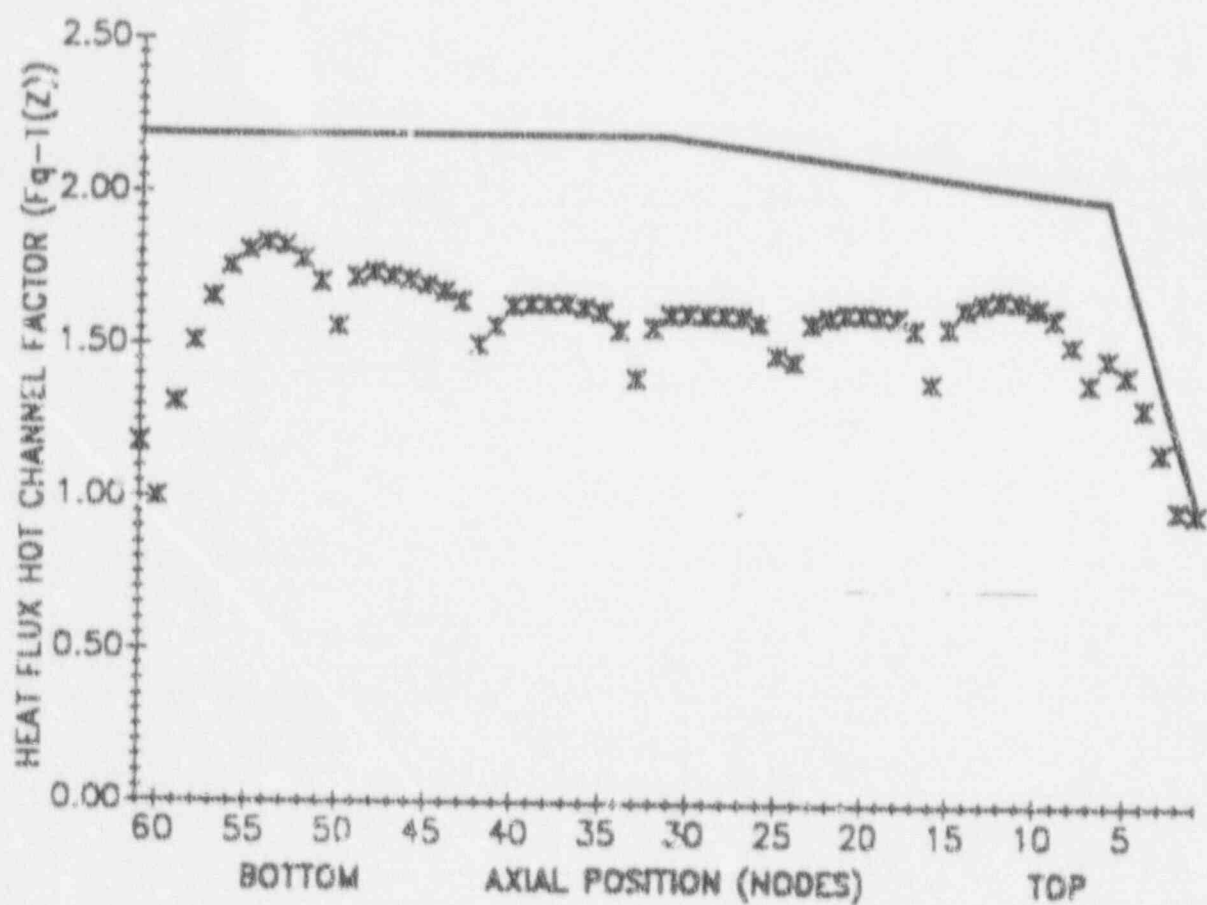
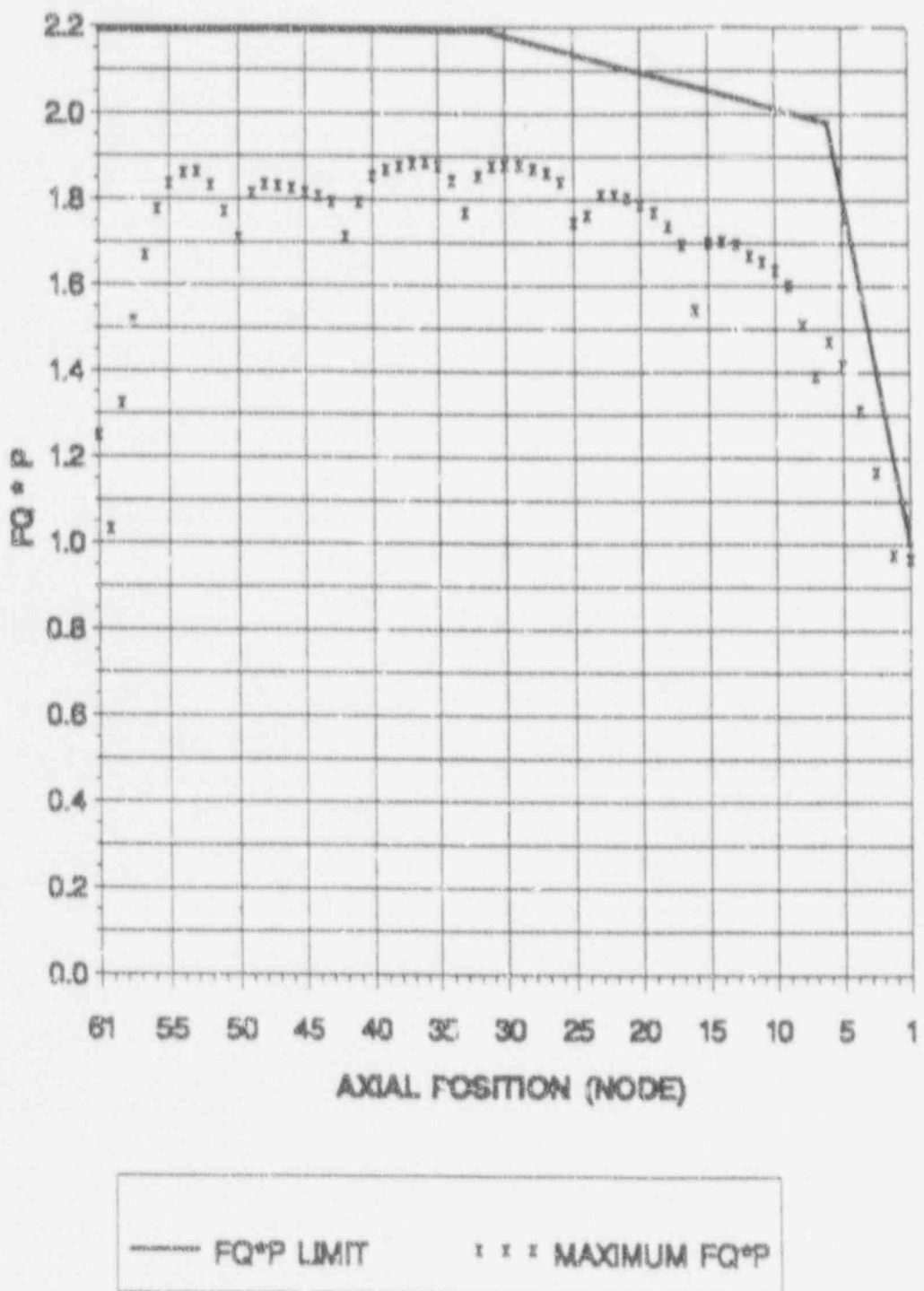


Figure 4.8
NORTH ANNA Unit 2 - CYCLE 8
MAXIMUM HEAT FLUX HOT CHANNEL FACTOR, $F_0(z)^*P$, vs. AXIAL POSITION



BOTTOM OF CORE

TOP OF CORE

Figure 4.9
NORTH ANNA Unit 2 - CYCLE 8
MAXIMUM HEAT FLUX HOT CHANNEL FACTOR, $F_Q(Z)$, vs. BURNUP

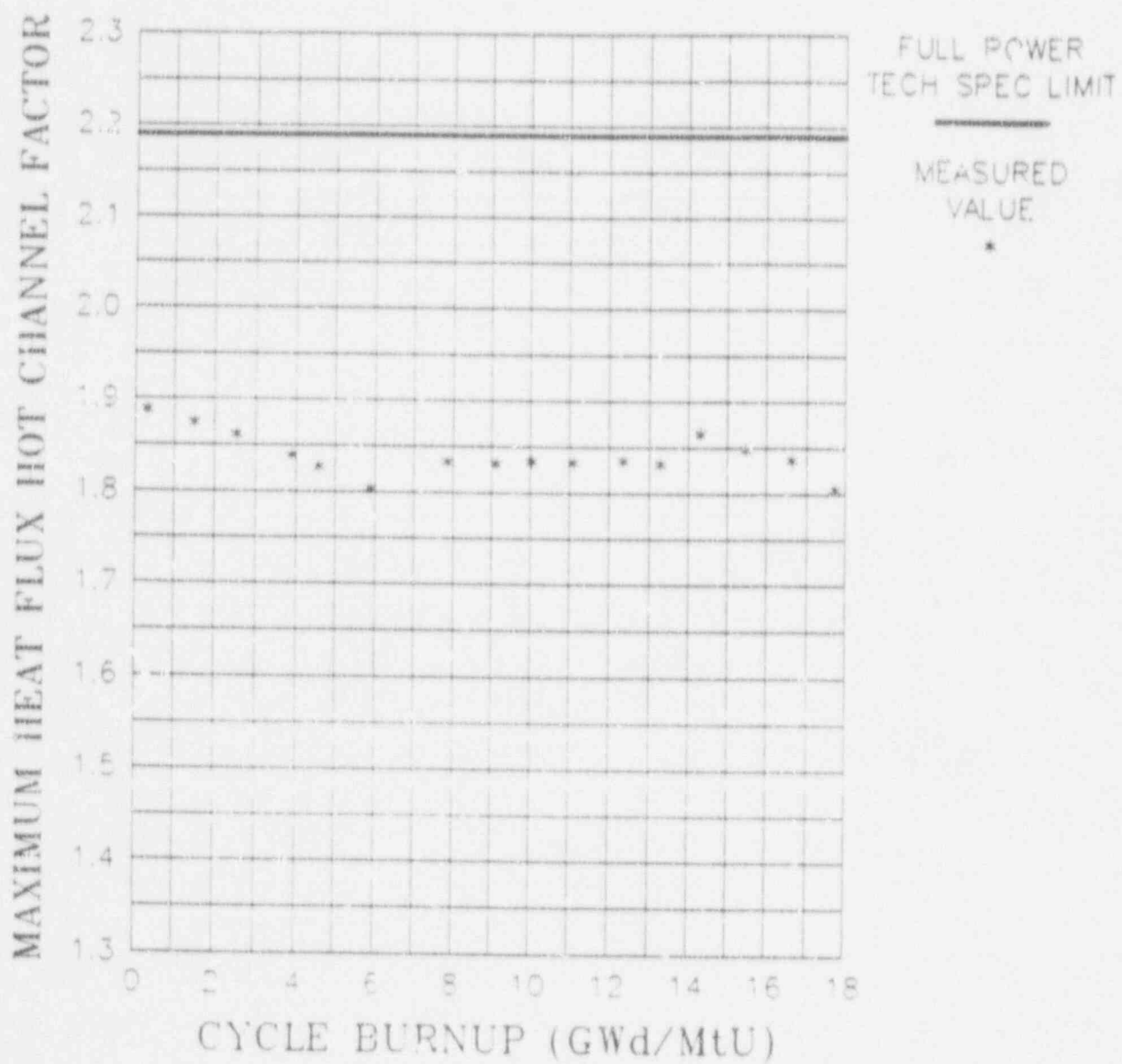


Figure 4.10
NORTH ANNA Unit 2 - CYCLE 8
MAXIMUM ENTHALPY RISE HOT CHANNEL FACTOR, $F_{\delta H}$, vs. BURNUP

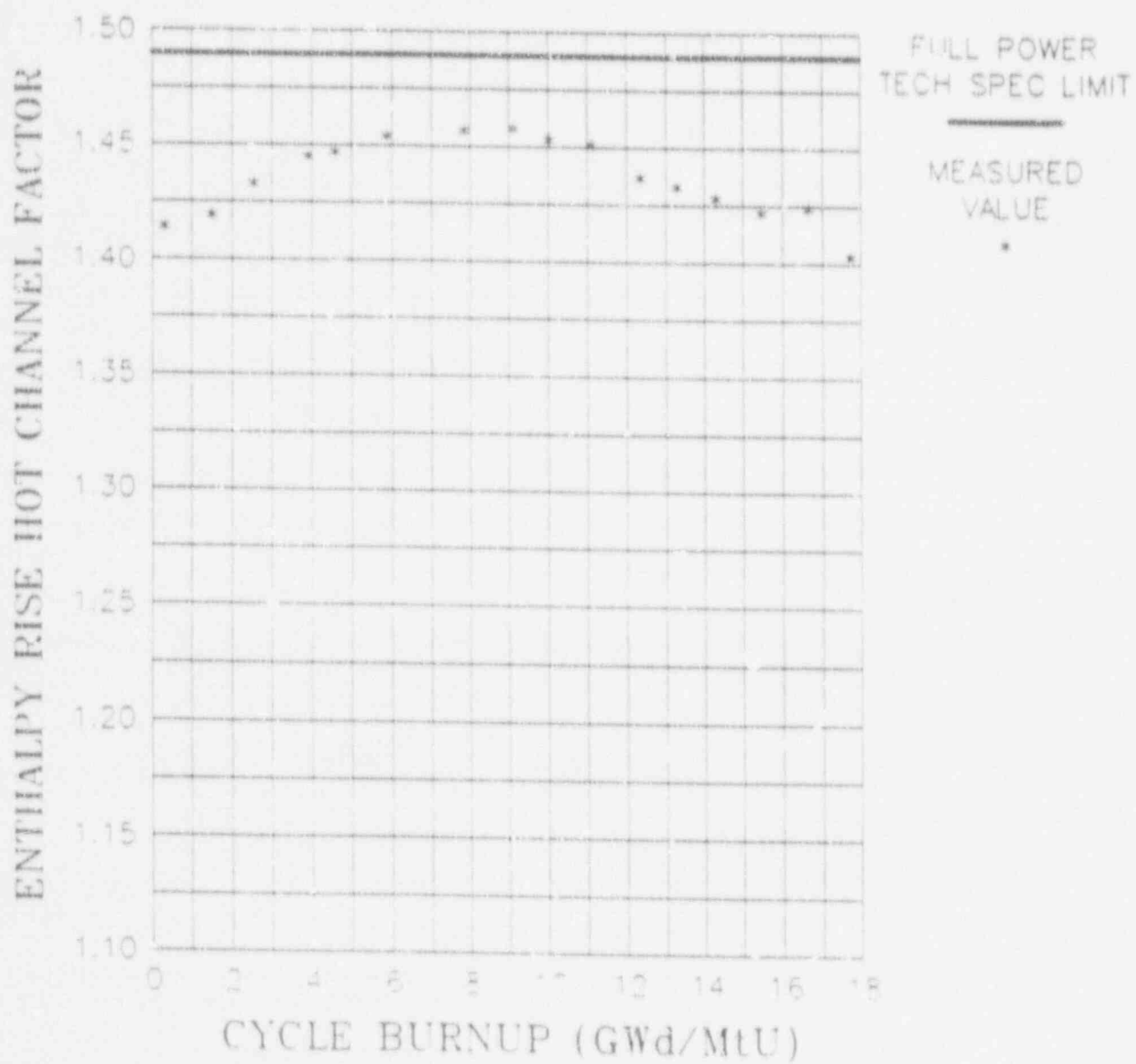


Figure 4.11
NORTH ANNA Unit 2 - CYCLE 8
TARGET DELTA FLUX vs. BURNUP

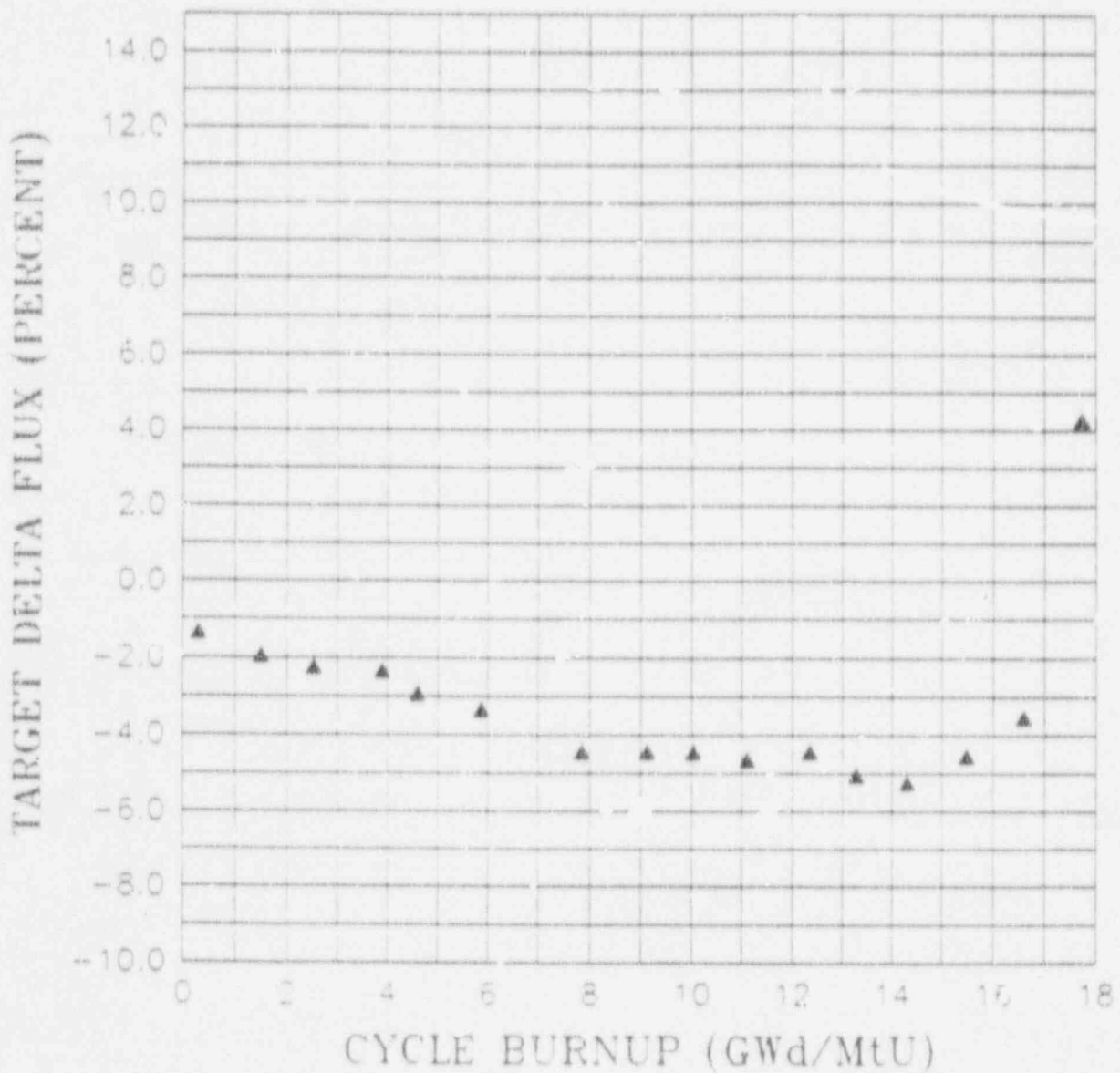


Figure 4.12
NORTH ANNA Unit 2 - CYCLE 8
CORE AVERAGE AXIAL POWER DISTRIBUTION
N2-8-07

$F_z \approx 1.208$
AXIAL OFFSET = -2.008

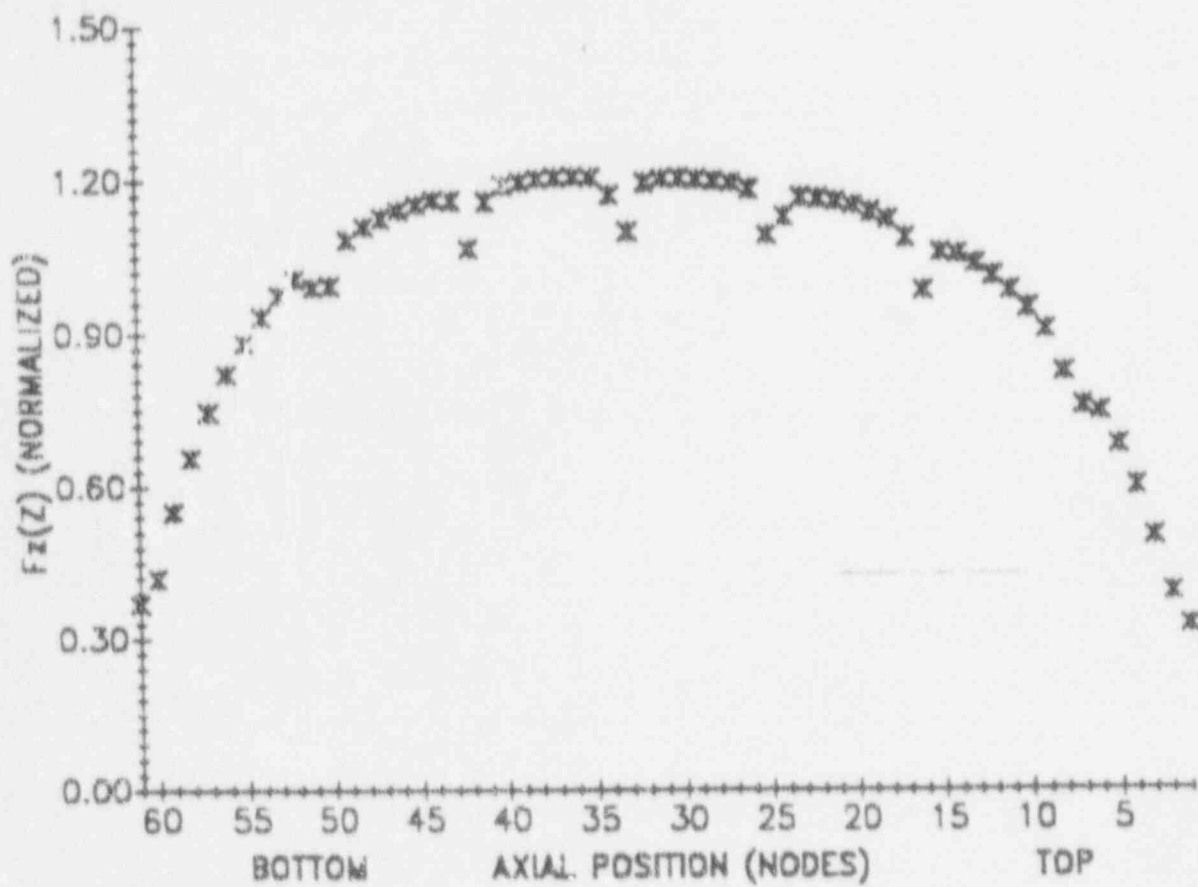


Figure 4.13
NORTH ANNA Unit 2 - CYCLE 8
CORE AVERAGE AXIAL POWER DISTRIBUTION
N2-8-14

$F_z = 1.157$
AXIAL OFFSET = +4.532

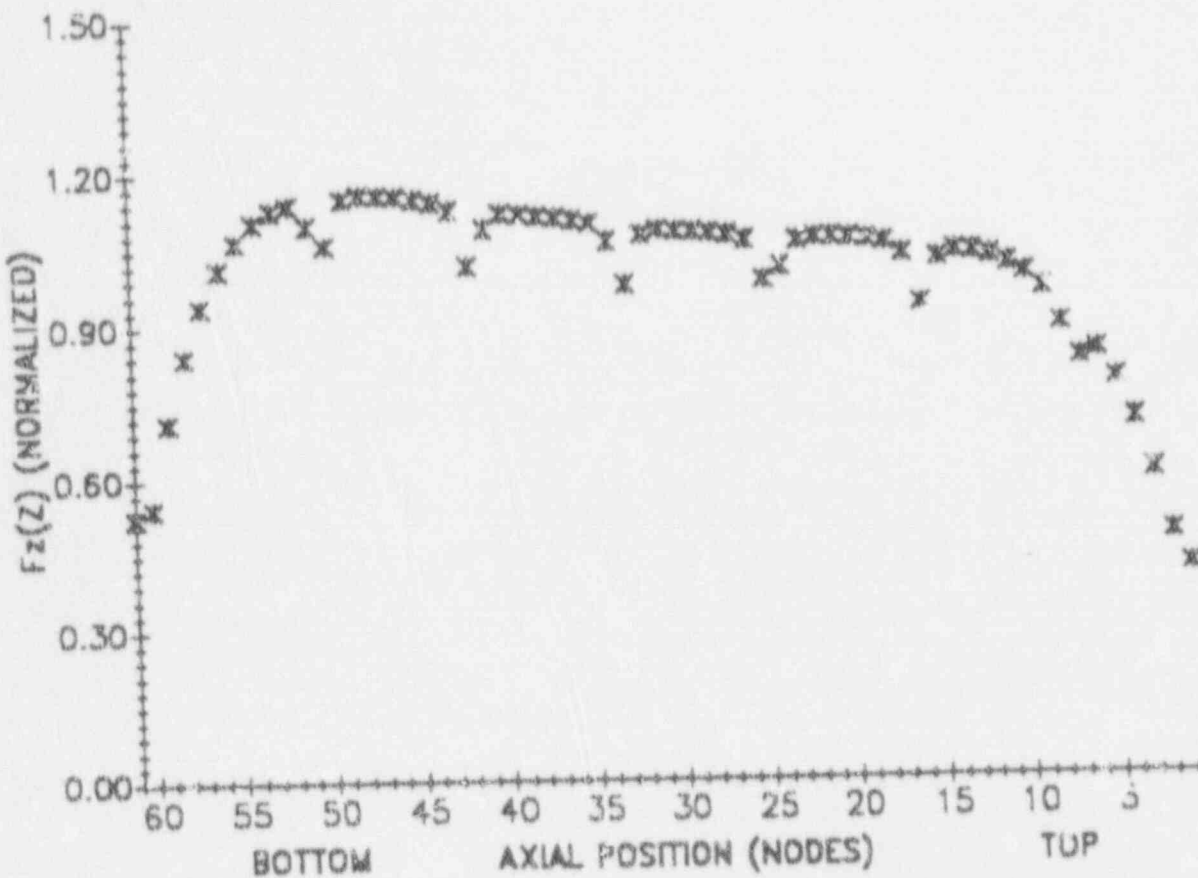


Figure 4.14
NORTH ANNA Unit 2 - CYCLE 8
CORE AVERAGE AXIAL POWER DISTRIBUTION
N2-8-25

$F_z \approx 1.157$
AXIAL OFFSET = -3.573

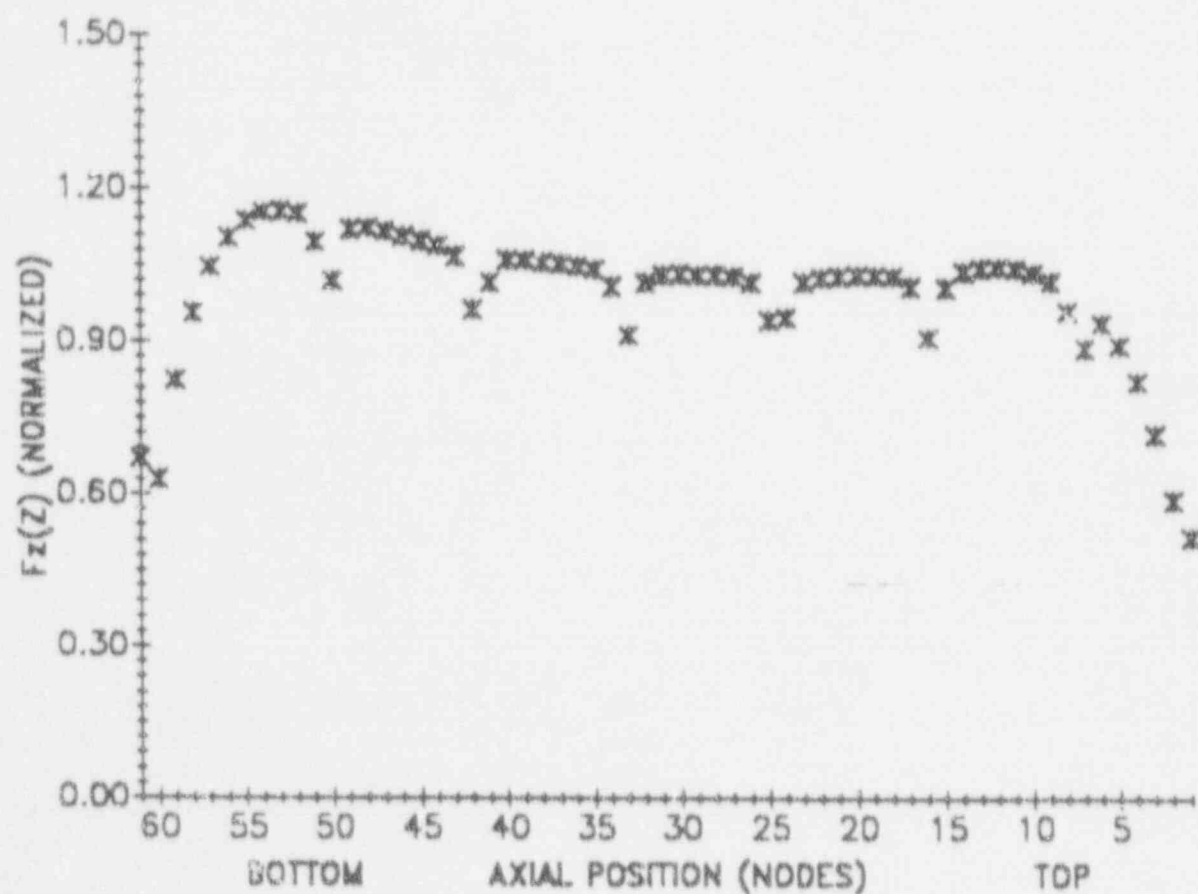
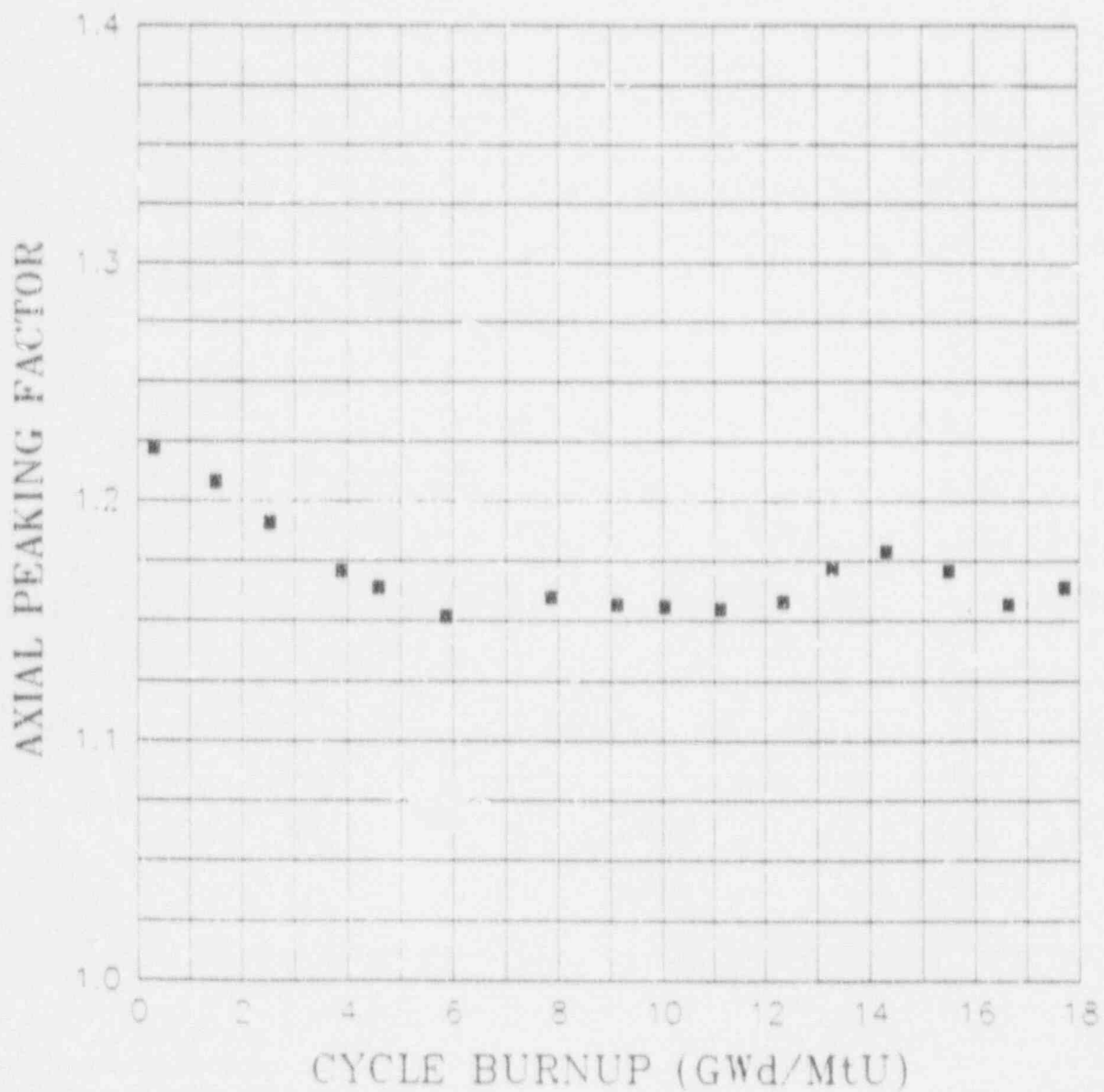


Figure 4.15
NORTH ANNA Unit 2 - CYCLE 8
CORE AVERAGE AXIAL PEAKING FACTOR vs. BURNUP



Section 5

PRIMARY COOLANT ACTIVITY

The specific activity levels of radioiodines in the primary coolant are important to core and fuel performance as indicators of failed fuel and are important with respect to offsite dose calculations associated with accident analyses.

Two mechanisms are responsible for the presence of radioiodines in the primary coolant. Radioiodines are always present due to direct fission product recoil from trace fissile materials plated onto core components and fuel structured surfaces or trace fissile materials existing as impurities in core structural materials. This fissile material is generally referred to as "tramp" material, and the resulting iodines are referred to as tramp iodine. Fission products will also diffuse into the primary coolant if a breach in the cladding (fuel defects) exists. Fuel defects are generally the predominant source of radioiodines in the primary coolant.

North Anna 2 Technical Specification 3.4.8 limits the radioiodines in the primary coolant to a dose equivalent I-131 value of 1.0 $\mu\text{Ci}/\text{gm}$ for modes one through five, inclusive. Figure 5.1 shows the dose-equivalent I-131 activity history for Cycle 8. These data show that the dose equivalent I-131 activity was substantially below the 1.0 $\mu\text{Ci}/\text{gm}$ limit for steady state power operation. The average full power equilibrium dose

equivalent I-131 concentration for the cycle was 2.42×10^{-2} $\mu\text{Ci/gm}$ which corresponds to less than 3% of the Technical Specification limit.

Correcting the I-131 concentration for tramp iodine involves calculating the I-131 activity from tramp fissile sources and subtracting this value from the measured I-131. The resultant is an estimate of the I-131 activity resulting directly from defective fuel. The magnitude of the tramp-corrected I-131 can be used as an indication of the number of defective fuel rods. The cycle average tramp corrected iodine-131 concentration was 1.57×10^{-2} $\mu\text{Ci/gm}$ with an average demineralizer flow rate of approximately 77 gpm during power operation. This magnitude of tramp corrected I-131 typically indicates the presence of defective fuel rods. Another positive indication of defective fuel is the presence of spikes in radioiodine during large or rapid power transients. Several iodine spikes can be seen on Figure 5.1.

The ratio of the specific activities of I-131 to I-133 is used to characterize the type (size) of fuel failure or failures which may have occurred in the reactor core. Use of the ratio for this determination is feasible because I-133 has a short half-life (approximately 21 hours) compared to that of I-131 (approximately eight days). For pinhole defects, where the diffusion time through the defect is on the order of days, the I-133 decays leaving the I-131 dominant in activity, thereby causing the ratio to be roughly 0.5 or more. In the case of larger leaks and tramp material, where the diffusion mechanism is negligible, the I-131/I-133 ratio will generally be less than 0.1. The use of these

ratios with regard to defect size is empirically determined and generally used throughout the commercial nuclear power industry.

Figure 5.2 shows the I-131/I-133 ratio data for North Anna 2 Cycle 8. Aside from the large increases in the ratio during the time when the defects occurred, the I-131/I-133 ratio settled out below a ratio of 0.5 toward the middle and end of cycle. This indicates that the defects in the cladding were likely to be moderately sized.

Fuel ultrasonic testing was performed during the Cycle 8 to Cycle 9 refueling outage. Eight fuel rods in five fuel assemblies were confirmed to be defective. The five fuel assemblies are X49, Y39, Y40, Y42, Y47. Assembly X49 was used for two cycles. Visual confirmation of the defective rod showed a through-wall defect on a corner rod below the bottom grid. This defect appears to be externally generated, but it is not clear whether debris or some other external mechanism induced the primary defect. Extensive hydriding was also observed toward the upper spans of this rod. Assemblies Y39, Y40, Y42, and Y47 are all from the new fuel batch for Cycle 8. No evidence of debris induced failures was found during the visual examination of these assemblies. There was evidence of hydriding of the fuel cladding just above the bottom grid on the failed fuel rods that were visible. Possible failure mechanisms are currently being evaluated with the fuel vendor (Westinghouse). These fuel assemblies will be restricted from further use pending any repair projects to replace the defective fuel rods.

Figure 5.1
NORTH ANNA UNIT 2 - C. LE 8
DOSE EQUIVALENT I-131 vs. TIME

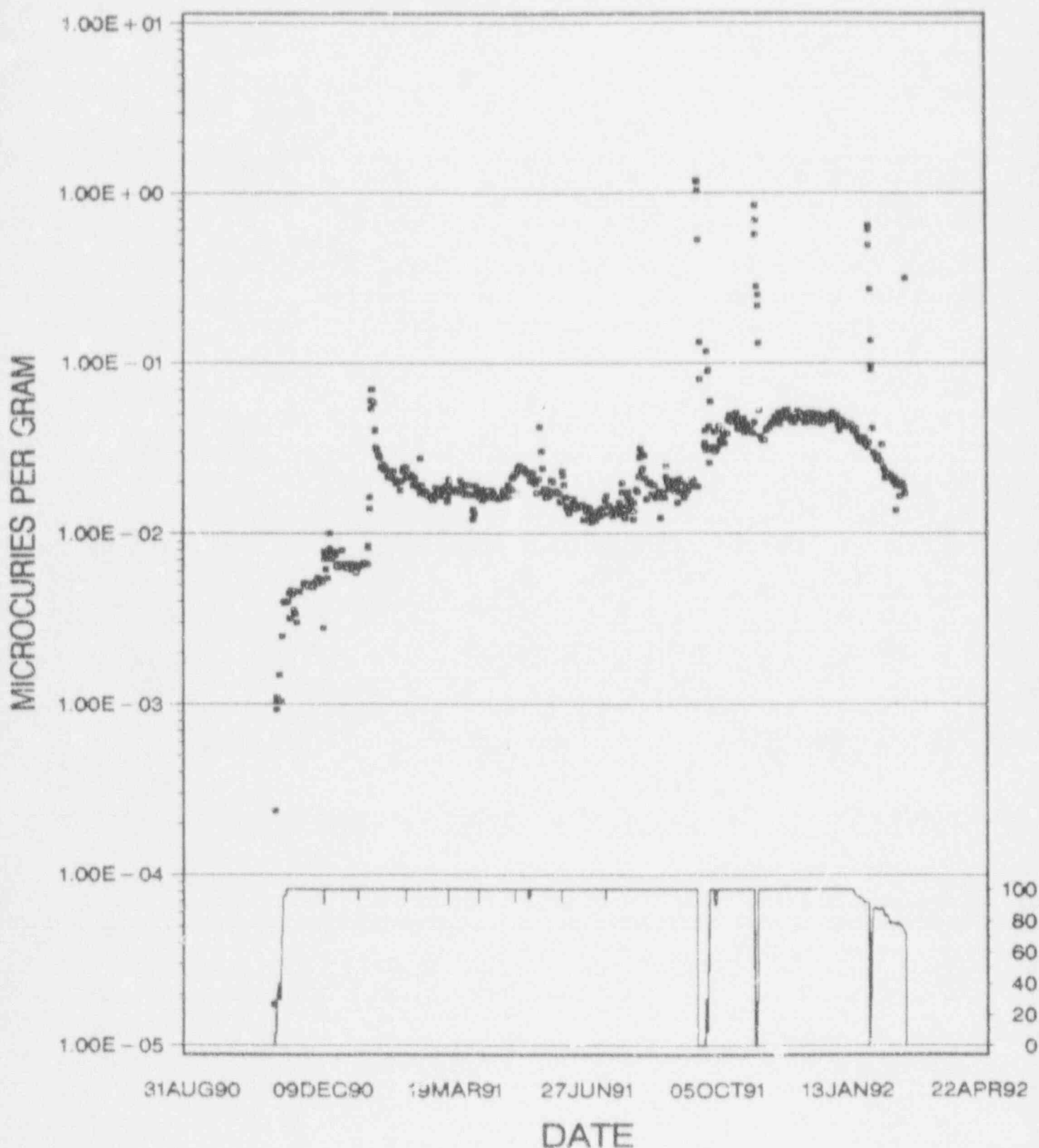
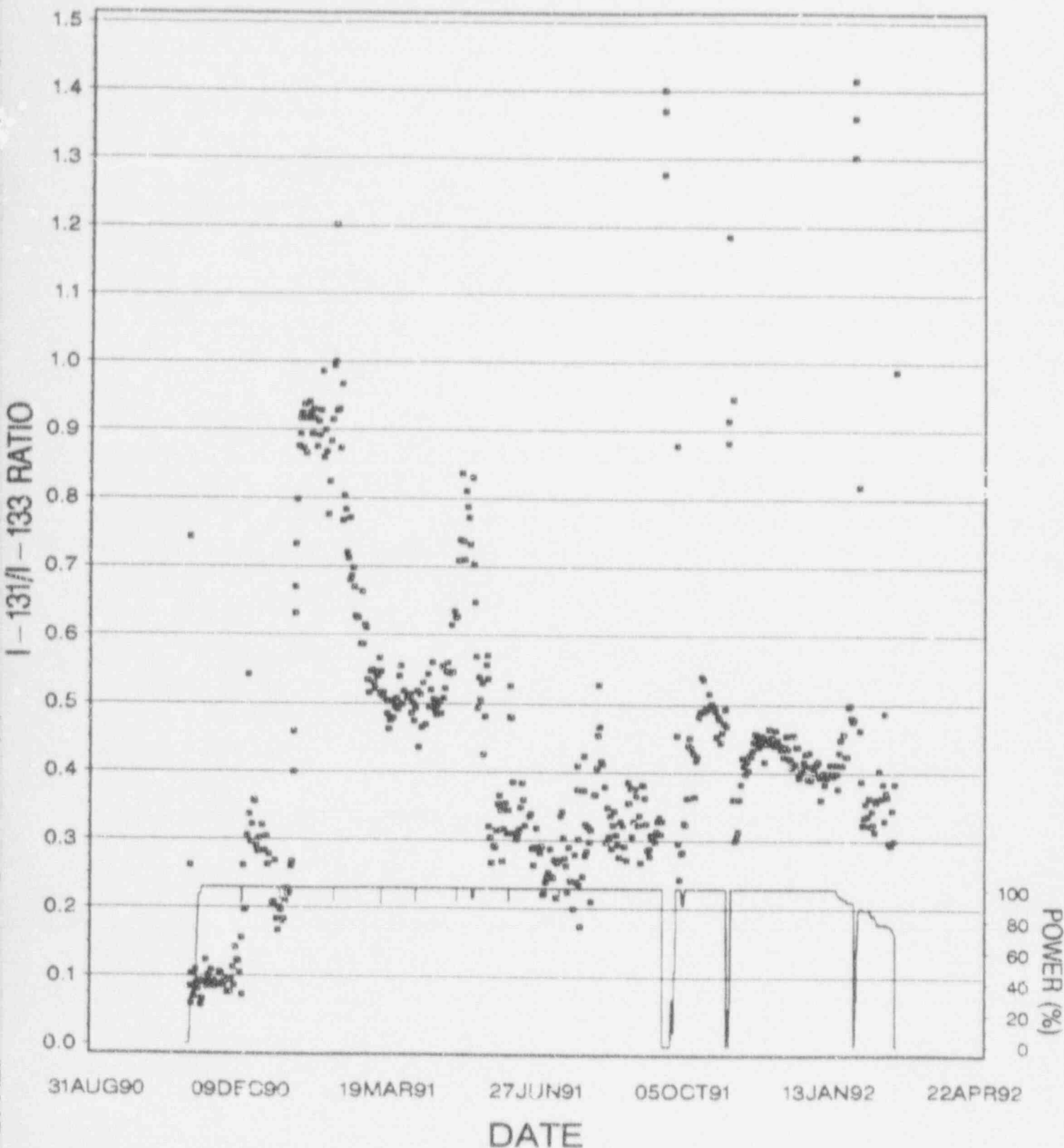


Figure 5.2
NORTH ANNA UNIT 2 - CYCLE 8
 $I-131 / I-133$ ACTIVITY RATIO vs. TIME



Section 6

CONCLUSIONS

The North Anna 2, Cycle 8 core has completed operation. Throughout this cycle, all core performance indicators compared favorably with the design predictions and the core related Technical Specifications limits were met with significant margin. No significant abnormalities in reactivity or burnup accumulation were detected. Radioiodine analysis indicated that there were apparent fuel rod defects during Cycle 8. During ultrasonic testing of the fuel, eight fuel rods in five fuel assemblies were determined to be defective. One of the five fuel assemblies was used for two cycles of operation. The remaining four assemblies were used only one cycle. These five assemblies will be restricted from further use pending repair.

Section 7

REFERENCES

- 1) E. A. Hoffman, "North Anna Unit 2, Cycle 8 Startup Physics Test Report," NE-817, January, 1991.
- 2) North Anna Power Station Junit 2 Technical Specifications, Sections 3/4.1, 3/4.2 and 3/4.4.8.
- 3) T. K. Ross, "NEWTOTE Code", VEPCO NFO-CCR-F , Rev. 9, April, 1984.
- 4) R. D. Klatt, W. D. Leggett, III, and L. D. Eisenhart, "FOLLOW Code," WCAP-7482, February, 1970.
- 5) W. D. Leggett, III and L. D. Eisenhart, "INCORE Code," WCAP-7149, December, 1967.
- 6) Memorandum from R. G. McAndrew to J. R. Hayes, "Core Operating Limits Report (COLR) Tech Spec Amendment 146/130", July 5, 1991.
- 7) T. T. Nguyen, "North Anna 2, Cycle 8 FOLLOW Input and Calculations", PM-363, Rev. 0, Addendum B, May 1992.